Supplemental information

Well-regulated Structures Featured Giant-molecule Acceptors Enable Long-term Stability and High-Performance Binary Organic Solar Cells

Jingyu Shi[1,2], *Pengfei Ding*[1,2], *Jintao Zhu*[3], *Zhenyu Chen*[1,2], *Shuangjiao Gao*[1], *Xueliang Yu*[1], *Xiaochun Liao*[1,2], *Quan Liu*[1], *Ziyi Ge*[1,2,*]

1. Materials

PM6 was purchased from Solarmer Energy Inc.

4,7-dibromo-5,6-dinitrobenzo[c][1,2,5]thiadiazole, tributyl(6-octylselenopheno [3,2-b] thiophen-2-yl) stannane, tributyl(6-octylthieno[3,2-b]thiophen-2-yl)stannane, 1-Bromo-3-octyldodecane, 2-(5-bromo-3-oxo-2,3-dihydro-1H-inden-1-ylidene) malononitrile, 2,5-bis-trimethylstannyl-thiophene, 2,5-bis-trimethylstannyl-selenophen and 2-(5,6-difluoro-3-oxo-2,3-dihydro-1H-inden-1-ylidene) malononitrile were purchased from Nanjing Zhiyan Technology Co., Ltd.

The ITO glass was purchased from Suzhou Shangyang Solar Technology Co., Ltd. All reagents were directly used without any further treatment, and all the reactions were carried out under a nitrogen atmosphere.

2. The synthetic routes of four GMAs, GMA-SSS, GMA-SSeS, GMA-SeSSe and GMA-SeSeSe.

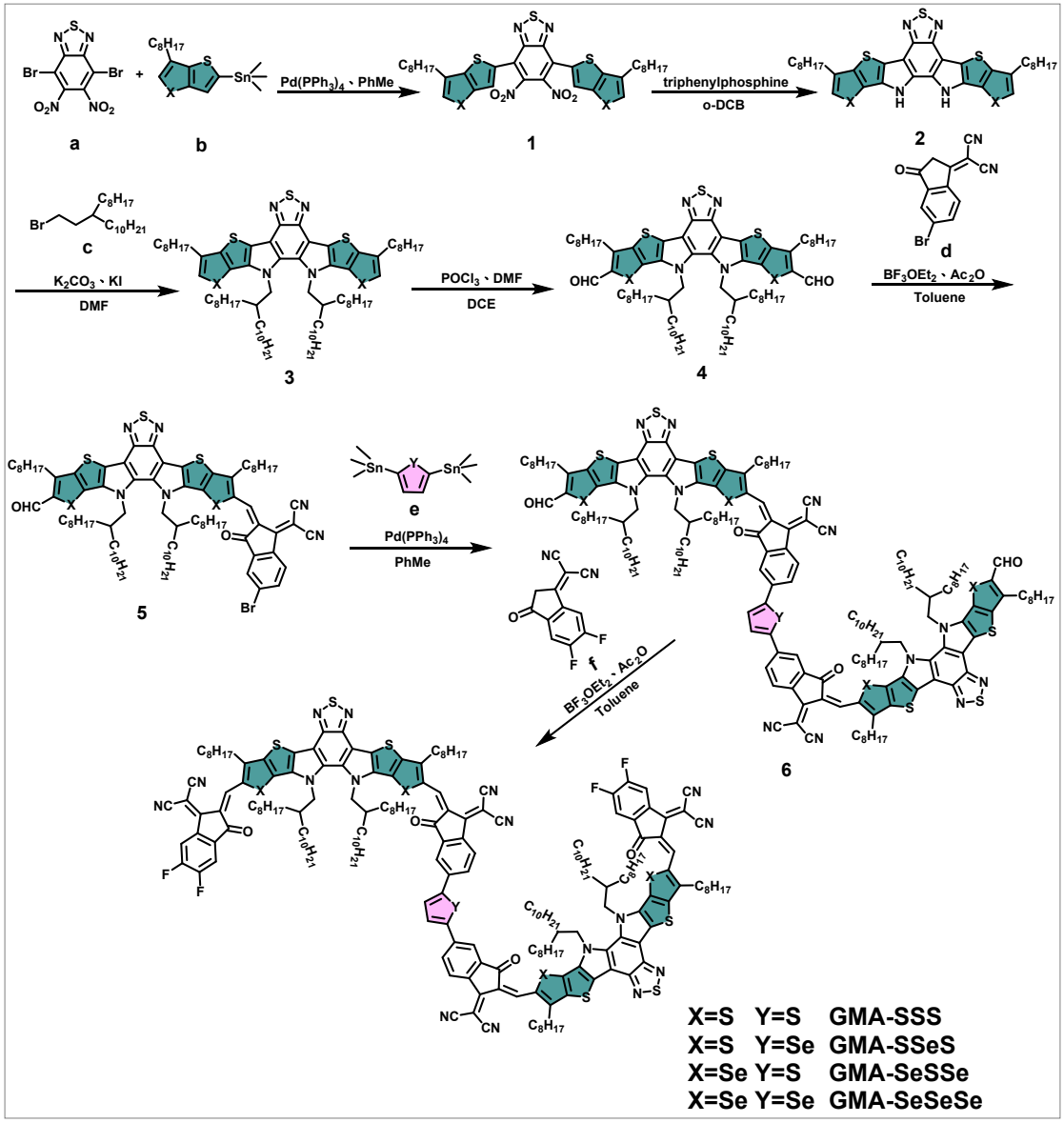

Figure S1. Synthetic routes of four GMAs.

Synthesis of compound 1 (X=Se), Compound **a** (4,7-dibromo-5,6-dinitrobenzo[c] [1,2,5]thiadiazole) (1.54 g, 4.00 mmol), compound **b** (tributyl(6-octylselenopheno [3,2-b] thiophen-2-yl) stannane) (5.88 g, 10.00 mmol) and $Pd(PPh_3)_4$ (0.23 g, 0.2 mmol) were dissolved in toluene (30 ml) and stirred at 110 ℃ for 5 h under nitrogen atmosphere. The solvent was removed under vacuum after the reaction mixture was cooled to ambient temperature. Compound **1 (X=Se)** were purified by chromatography in a silica gel column eluting with petroleum ether/dichloromethane (5/1, v/v), which yielding a red powder as product **1 (X=Se)** (2.26 g, 80% yield).

^{1}H NMR ($CDCl_3$): 7.75 (s, 2H), 7.71 (s, 2H), 2.75 (t, J=7.7 Hz, 4H), 1.84-1.74 (m, 4H), 1.42-1.26 (m, 20H), 0.92-0.86 (m, 6H).

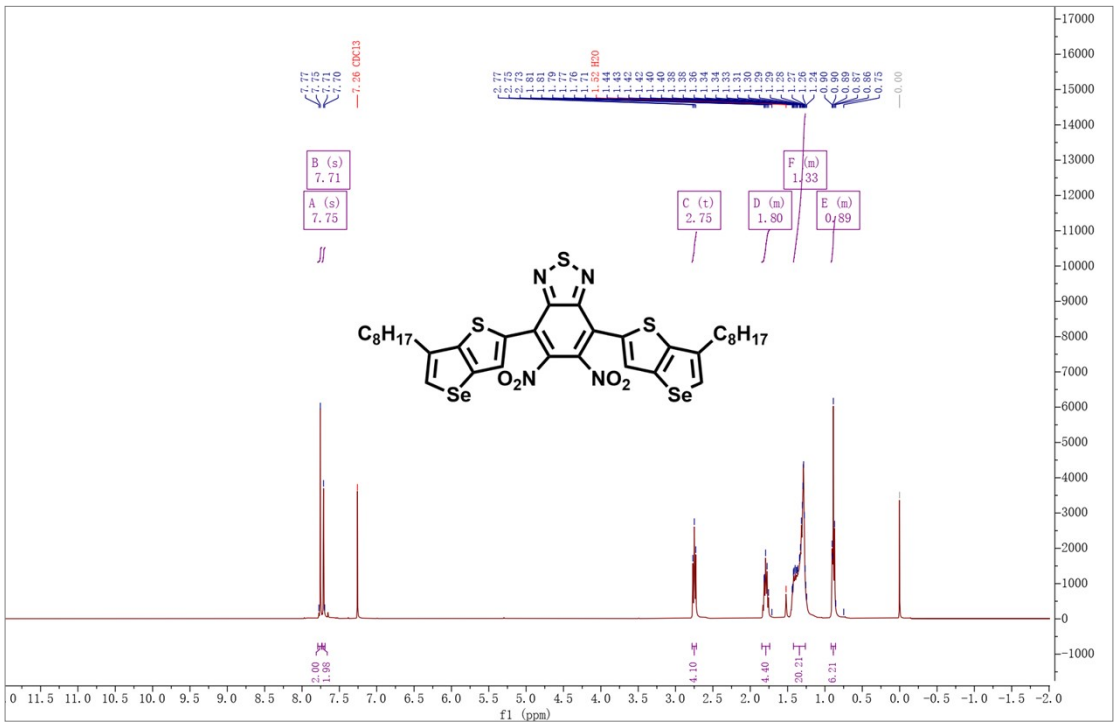

Figure S2. ^{1}H-NMR spectrum of compound **1 (X=Se)**.

Synthesis of compound 3 (X=Se), under nitrogen, compound **1 (X=Se)** (2.63 g, 3.20 mmol) and triphenylphosphine (9.03 g, 32.00 mmol) were dissolved in 1,2-dichlorobenzene (*o*-DCB, 35 ml). The mixture was stirred at 185 ℃ for 40 h. After cooled to ambient temperature, the solvent was removed under reduced pressure, which produced a red solid. The red intermediate **2 (X=Se)** was firstly washed with petroleum ether by column chromatography in a silica gel column, then washed with ethyl acetate. Compound **2 (X=Se)** (2.27 g, 3.00 mmol), compound **c** (1-Bromo-3-octyldodecane (5.50 g, 18.00 mmol)), K_2CO_3 (4.15 g, 30.00 mmol), KI (0.25 g, 1.50 mmol) and DMF (30 ml) were added into a three-necked round bottom flask. The mixture was deoxygenated with nitrogen for 3 min. The mixture was refluxed at 85 °C for 10 h. After removing the solvent from the filtrate, the residue was extracted with dichloromethane and H_2O. The mixture was purified with column chromatography on silica gel using petroleum ether/dichloromethane (3/1, v/v) as the eluent to give an orange solid **3 (X=Se)** (1.38 g, 35% yield).

^{1}H NMR ($CDCl_3$): 7.53 (s, 2H), 4.55 (d, J=7.8 Hz, 4H), 2.79 (t, J=7.8 Hz, 4H), 2.08 (p,

J=6.7 Hz, 2H), 1.86 (p, J=7.6 Hz, 4H), 1.47 (dt, J=12.0, 6.8 Hz, 4H), 1.32 (tdd, J=24.6, 12.2, 6.5 Hz, 22H), 1.18 (dt, J=13.9, 7.0 Hz, 12H), 1.10-0.92 (m, 30H), 0.85 (dt, J=20.9, 7.0 Hz, 28H), 0.75-0.62 (m, 6H).

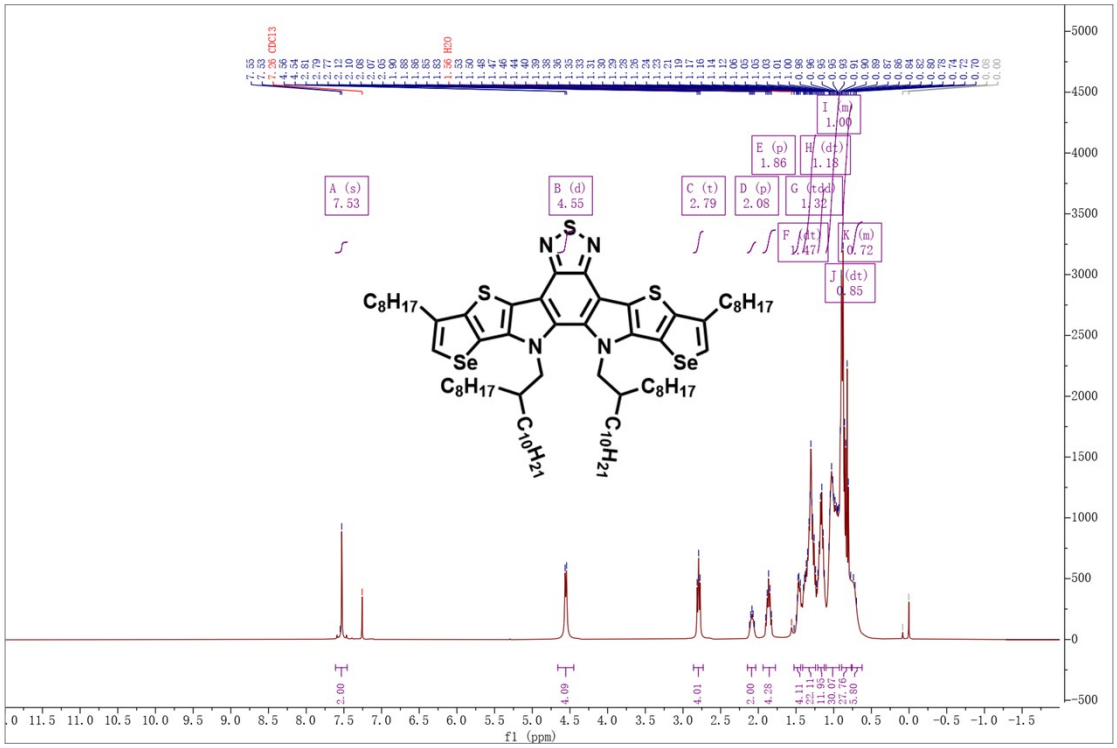

Figure S3. ^{1}H-NMR spectrum of compound **3 (X=Se)**.

Synthesis of compound 4 (X=S), a solution of compound **3 (X=S)** (1.29 g, 1.05 mmol) in 1,2-dichloroethane (DCE, 30 ml) was added in a three-neck flask under nitrogen. The anhydrous DMF (0.8 ml) and phosphorus oxychloride (0.8 ml) was added at 0 ℃ (icy water bathing), the mixture was then stirred for 2 h. After withdrew the ice bath, the mixture was heated to 85 ℃ and reacted overnight. The mixture was poured into saturated sodium carbonate aqueous solution (300 ml) to quench the reaction and extracted with dichloromethane several times. Removing the solvent and the crude product was purified by column chromatography in a silica gel column, eluting with petroleum ether/dichloromethane (2/1, v/v) to give compound **4 (X=S)** (orange solid, 1.21 g, 90% yield).

^{1}H NMR ($CDCl_3$): 10.14 (s, 2H), 4.62 (d, J=7.8 Hz, 4H), 3.19 (t, J=7.8 Hz, 4H), 2.04 (q, J=6.3 Hz, 2H), 1.91 (q, J=7.7 Hz, 4H), 1.50-1.44 (m, 4H), 1.38 (q, J=5.0, 3.1 Hz, 4H), 1.36-1.24 (m, 18H), 1.23-1.09 (m, 16H), 1.08-0.90 (m, 36H), 0.88 (d, J=1.6 Hz, 4H), 0.82 (d, J=7.1 Hz, 6H), 0.79 (s, 4H).

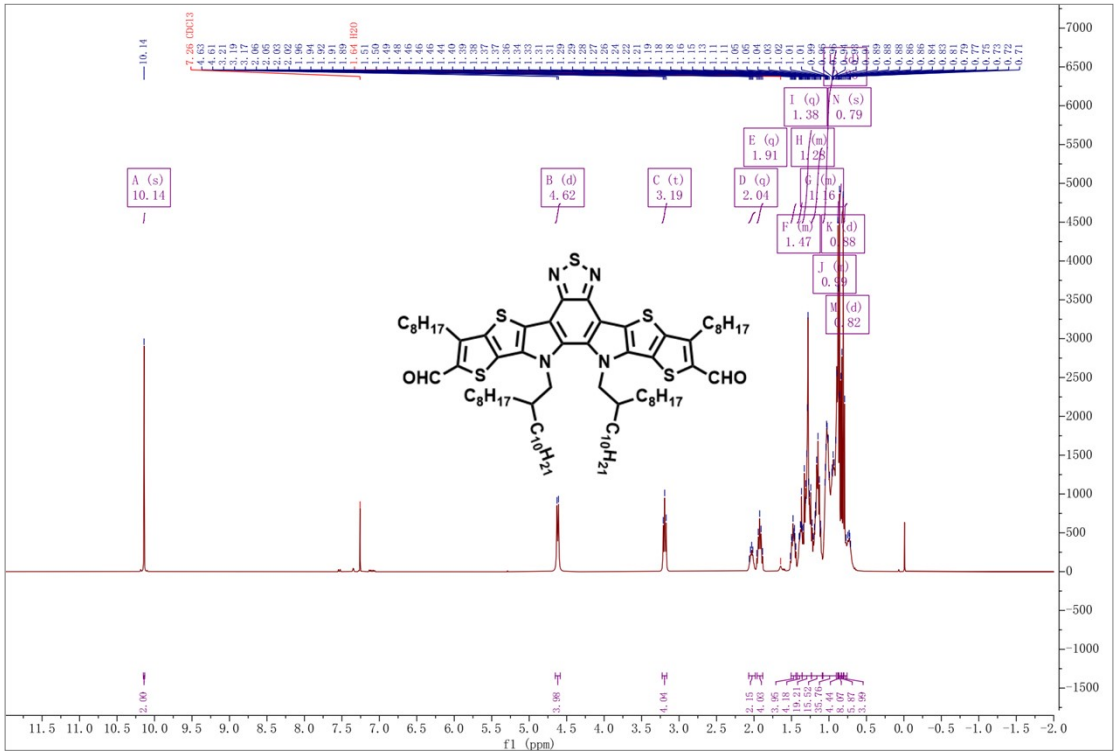

Figure S4. ^{1}H-NMR spectrum of compound **4 (X=S)**.

Synthesis of compound 4 (X=Se), a solution of compound **3 (X=Se)** (1.38 g, 1.05 mmol) in 1,2-dichloroethane (DCE, 30 ml) was added in a three-neck flask under nitrogen. The anhydrous DMF (0.8 ml) and phosphorus oxychloride (0.8 ml) was added at 0 ℃ (icy water bathing), the mixture was then stirred for 2 h. After withdrew the ice bath, the mixture was heated to 85 ℃ and reacted overnight. The mixture was poured into saturated sodium carbonate aqueous solution (300 ml) to quench the reaction and extracted with dichloromethane several times. Removing the solvent and the crude product was purified by column chromatography in a silica gel column, eluting with petroleum ether/dichloromethane (2/1, v/v) to give compound **4 (X=Se)** (orange solid, 1.30 g, 90% yield).

^{1}H NMR ($CDCl_3$): 10.04 (s, 2H), 4.59 (d, J=7.7 Hz, 4H), 3.18 (t, J=7.8 Hz, 4H), 2.03 (q, J=6.4 Hz, 2H), 1.94 (q, J=7.6 Hz, 4H), 1.48 (q, J=7.8 Hz, 4H), 1.38 (q, J=5.4, 3.7 Hz, 4H), 1.32-1.20 (m, 18H), 1.15 (p, J=6.5 Hz, 12H), 1.06-0.91 (m, 30H), 0.90-0.81 (m, 28H), 0.78-0.66 (m, 6H).

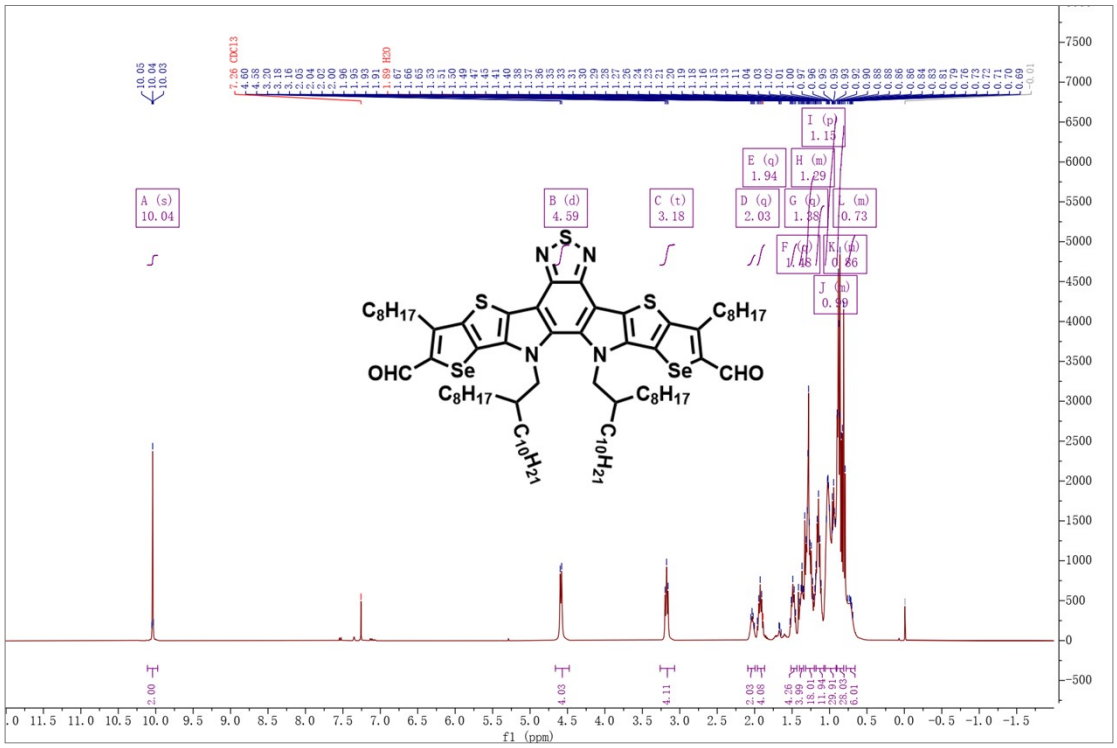

Figure S5. ^{1}H-NMR spectrum of compound **4 (X=Se)**.

Synthesis of compound 5 (X=S), under nitrogen, compound **4 (X=S)** (1.21 g, 0.95 mmol), compound **d** 2-(5-bromo-3-oxo-2,3-dihydro-1H-inden-1-ylidene) malononitrile (0.26 g, 0.95 mmol), BF_3OEt_2 (0.80 ml), acetic anhydride Ac_2O (1.00 ml) and toluene (15 ml) were added to a 50 ml round-bottled flask. After the reaction performed at 60 ℃ for 30 minutes, the mixture was poured into methanol and filtered. The residue was purified in a silica gel column using petroleum ether/chloroform (1.5/1, v/v) as the eluent. Compound **5 (X=S)** was obtained as a green solid (0.87 g, 60% yield).

^{1}H NMR ($CDCl_3$): 10.16 (s, 1H), 9.12 (s, 1H), 8.50 (d, J=8.4 Hz, 1H), 8.00 (s, 1H), 7.79 (d, J=8.5 Hz, 1H), 4.71 (dd, J=32.2, 7.7 Hz, 4H), 3.19 (dt, J=14.5, 7.8 Hz, 4H), 2.10 (h, J=6.7 Hz, 2H), 1.97-1.82 (m, 4H), 1.49 (h, J=7.4, 6.1 Hz, 4H), 1.38 (d, J=9.9 Hz, 4H), 1.29 (h, J=7.8, 7.2 Hz, 20H), 1.18-1.09 (m, 16H), 1.07-0.92 (m, 36H), 0.89 (s, 4H), 0.86 (dd, J=6.7, 3.8 Hz, 8H), 0.81 (d, J=2.6 Hz, 4H), 0.78 (d, J=7.5 Hz, 6H).

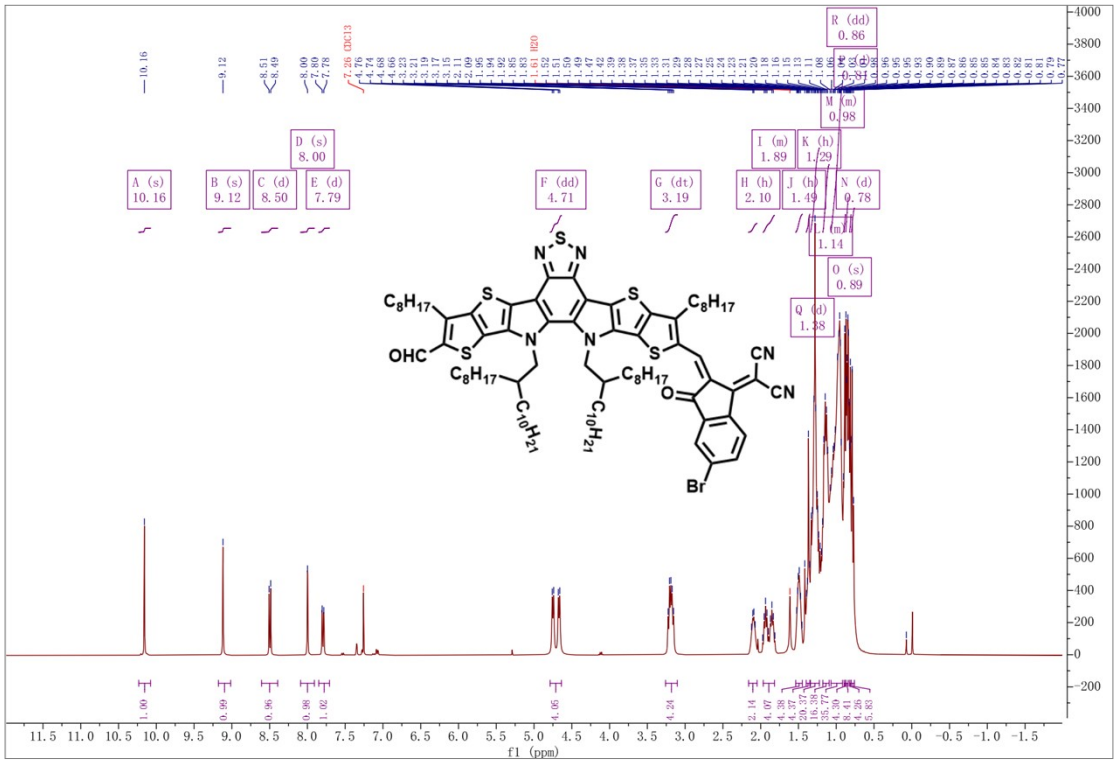

Figure S6. ^{1}H-NMR spectrum of compound **5 (X=S)**.

Synthesis of compound 5 (X=Se), under nitrogen, compound **4 (X=Se)** (1.30 g, 0.95 mmol), compound **d** 2-(5-bromo-3-oxo-2,3-dihydro-1H-inden-1-ylidene) malononitrile (0.26 g, 0.95 mmol), BF_3OEt_2 (0.80 ml), acetic anhydride Ac_2O (1.00 ml) and toluene (15 ml) were added to a 50 ml round-bottled flask. After the reaction performed at 60 ℃ for 30 minutes, the mixture was poured into methanol and filtered. The residue was purified in a silica gel column using petroleum ether/chloroform (1.5/1, v/v) as the eluent. Compound **5 (X=Se)** was obtained as a green solid (0.93 g, 60% yield).

^{1}H NMR ($CDCl_3$): 10.06 (s, 1H), 9.25 (s, 1H), 8.51 (d, J=8.4 Hz, 1H), 8.00 (d, J=1.8 Hz, 1H), 7.81 (d, J=8.4 Hz, 1H), 4.65 (dd, J=23.3, 7.7 Hz, 4H), 3.20 (q, J=7.9 Hz, 4H), 2.10 (h, J=6.6 Hz, 2H), 1.89 (dp, J=33.6, 7.8 Hz, 4H), 1.55-1.46 (m, 4H), 1.37 (d, J=5.0 Hz, 4H), 1.30 (dt, J=21.0, 9.0 Hz, 18H), 1.15 (dt, J=10.4, 6.5 Hz, 12H), 1.06 (ddd, J=18.6, 9.7, 4.2 Hz, 16H), 1.00-0.94 (m, 16H), 0.93-0.81 (m, 28H), 0.78 (d, J=7.5 Hz, 6H).

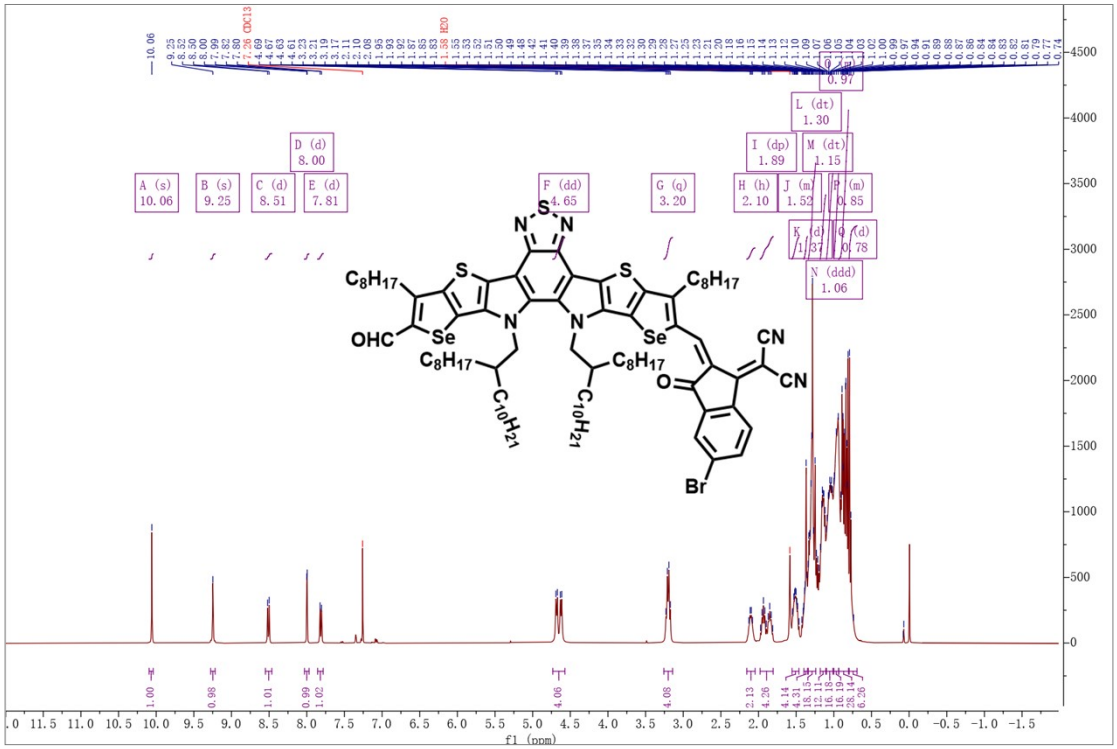

Figure S7. ^{1}H-NMR spectrum of compound **5 (X=Se)**.

Synthesis of compound 6 (X=S, Y=S) and GMA-SSS, compound **5 (X=S)** (0.44 g, 0.29 mmol), compound **e** (2,5-bis-trimethylstannyl-thiophene) (0.054 g, 0.13 mmol) and $Pd(PPh_3)_4$ (0.023 g, 0.02 mmol) were dissolved in toluene (20 ml) and stirred at 110 ℃ for 5 h under nitrogen atmosphere. The solvent was removed under vacuum after the reaction mixture was cooled to ambient temperature. Compound **6 (X=S, Y=S)** were purified by chromatography in a silica gel column eluting with petroleum ether/dichloromethane (1/1.5, v/v), which yielding a blue solid as product **6 (X=S, Y=S)** (0.27 g, 70% yield).

^{1}H NMR ($CDCl_3$): 10.17 (s, 2H), 9.15 (s, 2H), 8.75 (d, J=8.3 Hz, 2H), 8.12 (s, 2H), 7.99-7.91 (m, 2H), 7.62 (s, 2H), 4.73 (dd, J=33.8, 7.7 Hz, 8H), 3.21 (q, J=7.6 Hz, 8H), 2.12 (dt, J=12.6, 6.7 Hz, 4H), 1.91 (dt, J=26.5, 7.6 Hz, 8H), 1.49 (dd, J=14.7, 7.1 Hz, 8H), 1.42-1.35 (m, 8H), 1.35-1.20 (m, 40H), 1.14 (dt, J=17.8, 5.1 Hz, 32H), 1.08-0.92 (m, 72H), 0.89 (s, 8H), 0.88-0.84 (m, 16H), 0.83 (d, J=2.8 Hz, 8H), 0.81-0.76 (m, 12H).

Under nitrogen, compound **6 (X=S, Y=S)** (0.27 g, 0.09 mmol), compound **f** 2-(5,6-difluoro-3-oxo-2,3-dihydro-1H-inden-1-ylidene) malononitrile (0.083 g, 0.36 mmol), BF_3OEt_2 (0.40 ml), acetic anhydride Ac_2O (0.50 ml) and toluene (10 ml) were added to a 25 ml round-bottled flask. After the reaction performed at 60 ℃ for 30 minutes, the

mixture was poured into methanol and filtered. The residue was purified in a silica gel column using petroleum ether/chloroform (1/2, v/v) as the eluent. Compound **GMA-SSS** was obtained as a dark blue solid (0.28 g, 90% yield).

^{1}H NMR ($CDCl_3$): 9.08 (s, 4H), 8.69 (d, J=8.4 Hz, 2H), 8.59-8.49 (m, 2H), 8.04 (s, 2H), 7.90 (d, J=8.5 Hz, 2H), 7.66 (dd, J=14.4, 6.3 Hz, 4H), 4.96-4.74 (m, 8H), 3.18 (s, 8H), 2.33-2.18 (m, 4H), 1.87 (s, 8H), 1.52 (t, J=7.6 Hz, 8H), 1.40-1.35 (m, 8H), 1.29 (s, 40H), 1.18-1.12 (m, 32H), 1.07 (q, J=12.0, 11.0 Hz, 72H), 0.89 (t, J=6.3 Hz, 20H), 0.81 (q, J=8.8, 7.9 Hz, 24H).

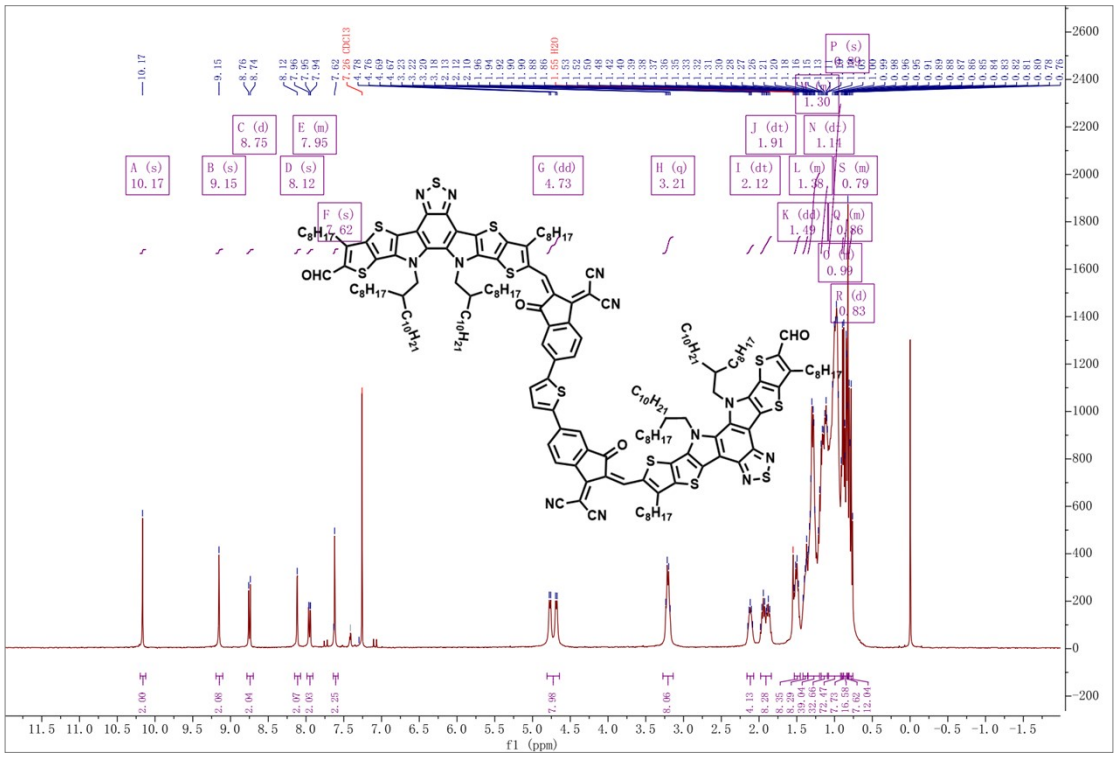

Figure S8. ^{1}H-NMR spectrum of compound **6 (X=S, Y=S)**.

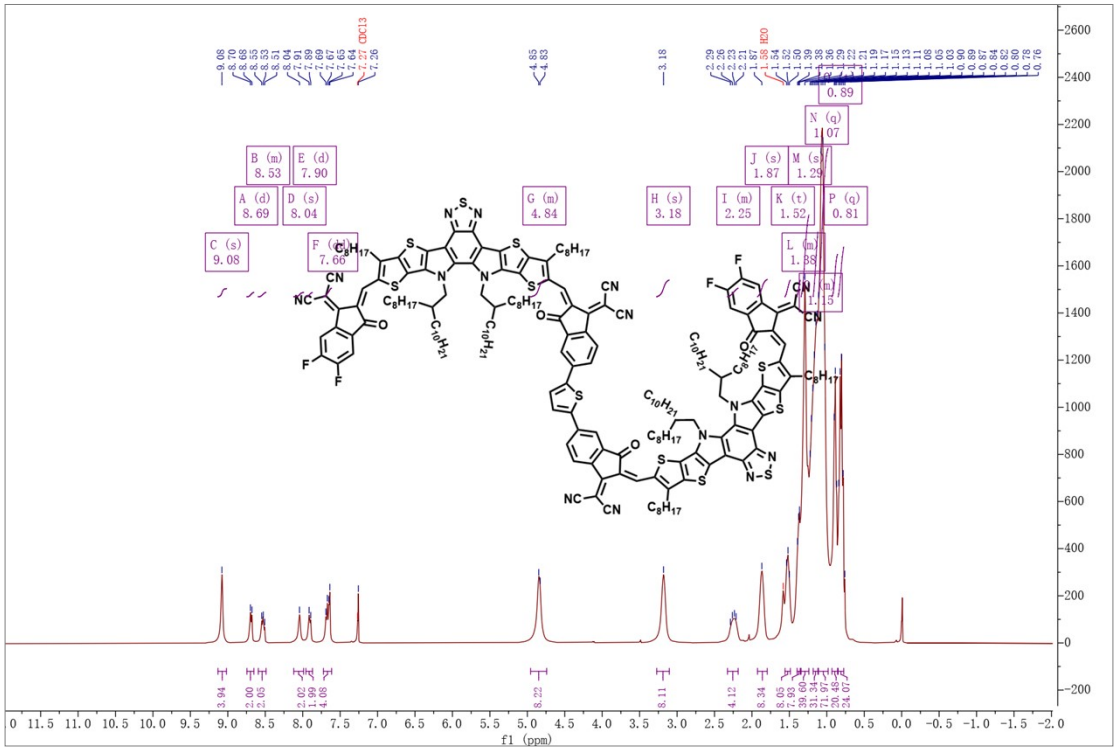

Figure S9. ^{1}H-NMR spectrum of compound **GMA-SSS**.

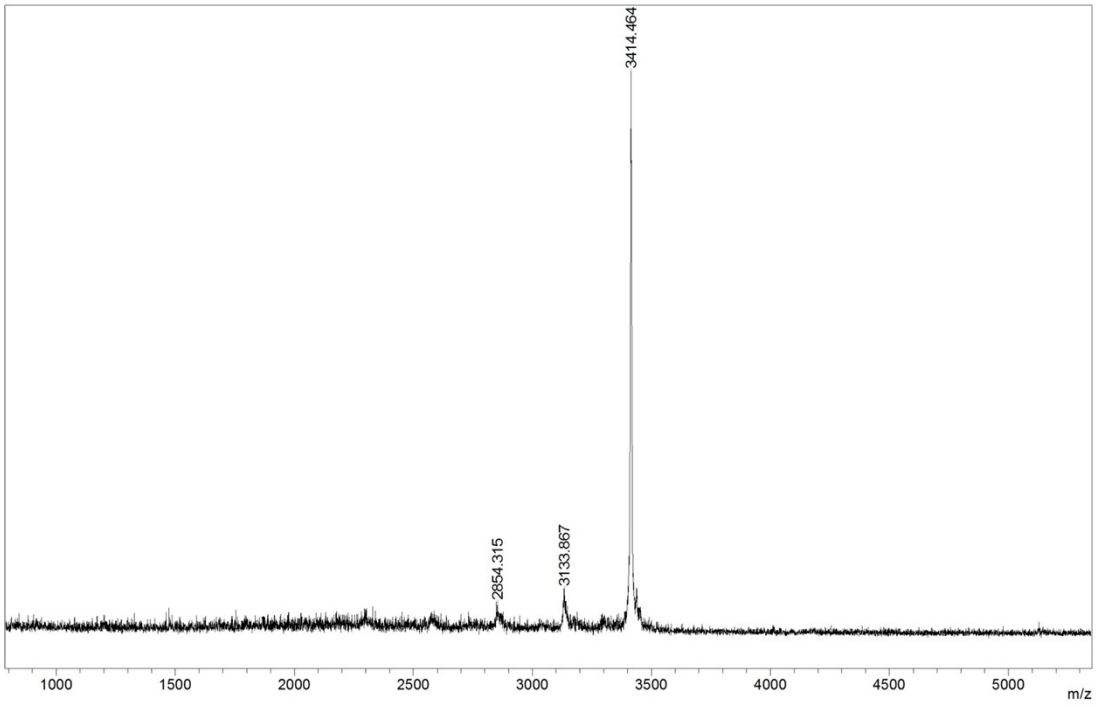

Figure S10. MALDI-TOF spectrum of **GMA-SSS**.

Synthesis of compound 6 (X=S, Y=Se) and GMA-SSeS, compound **5 (X=S)** (0.44 g, 0.29 mmol), compound **e** (2,5-bis-trimethylstannyl- selenophen) (0.059 g, 0.13 mmol) and $Pd(PPh_3)_4$ (0.023 g, 0.02 mmol) were dissolved in toluene (20 ml) and stirred at 110 ℃ for 5 h under nitrogen atmosphere. The solvent was removed under vacuum

after the reaction mixture was cooled to ambient temperature. Compound **6 (X=S, Y=Se)** were purified by chromatography in a silica gel column eluting with petroleum ether/dichloromethane (1/1.5, v/v), which yielding a blue solid as product **6 (X=S, Y=Se)** (0.28 g, 70% yield).

^{1}H NMR ($CDCl_3$): 10.17 (s, 2H), 9.10 (s, 2H), 8.69 (d, J=8.2 Hz, 2H), 8.03 (s, 2H), 7.89-7.74 (m, 4H), 4.75 (dd, J=33.4, 7.6 Hz, 8H), 3.19 (dt, J=25.8, 7.9 Hz, 8H), 2.15 (dq, J=13.6, 6.3 Hz, 4H), 1.90 (dt, J=37.7, 7.7 Hz, 8H), 1.50 (dd, J=8.9, 4.8 Hz, 8H), 1.38 (d, J=14.0 Hz, 8H), 1.29 (ddd, J=13.0, 10.8, 5.8 Hz, 32H), 1.13 (ddd, J=15.0, 7.5, 3.3 Hz, 40H), 1.08-0.92 (m, 72H), 0.90 (d, J=6.5 Hz, 8H), 0.86 (d, J=7.1 Hz, 16H), 0.83 (d, J=3.2 Hz, 8H), 0.78 (t, J=7.5 Hz, 12H).

Under nitrogen, compound **6 (X=S, Y=Se)** (0.28 g, 0.09 mmol), compound **f** 2-(5,6-difluoro-3-oxo-2,3-dihydro-1H-inden-1-ylidene) malononitrile (0.083 g, 0.36 mmol), BF_3OEt_2 (0.40 ml), acetic anhydride Ac_2O (0.50 ml) and toluene (10 ml) were added to a 25 ml round-bottled flask. After the reaction performed at 60 ℃ for 30 minutes, the mixture was poured into methanol and filtered. The residue was purified in a silica gel column using petroleum ether/chloroform (1/2, v/v) as the eluent. Compound **GMA-SSeS** was obtained as a dark blue solid (0.28 g, 90% yield).

^{1}H NMR ($CDCl_3$): 9.11 (d, J=8.7 Hz, 4H), 8.71 (d, J=8.0 Hz, 2H), 8.55 (dd, J=9.9, 6.4 Hz, 2H), 8.05 (s, 2H), 7.89 (d, J=8.3 Hz, 2H), 7.81 (s, 2H), 7.65 (t, J=7.5 Hz, 2H), 4.82 (d, J=7.8 Hz, 8H), 3.20 (t, J=8.0 Hz, 8H), 2.19 (s, 4H), 1.88 (q, J=7.5 Hz, 8H), 1.53 (t, J=7.7 Hz, 8H), 1.41-1.25 (m, 40H), 1.19-1.11 (m, 32H), 1.03 (d, J=10.3 Hz, 72H), 0.92-0.86 (m, 20H), 0.83-0.77 (m, 24H).

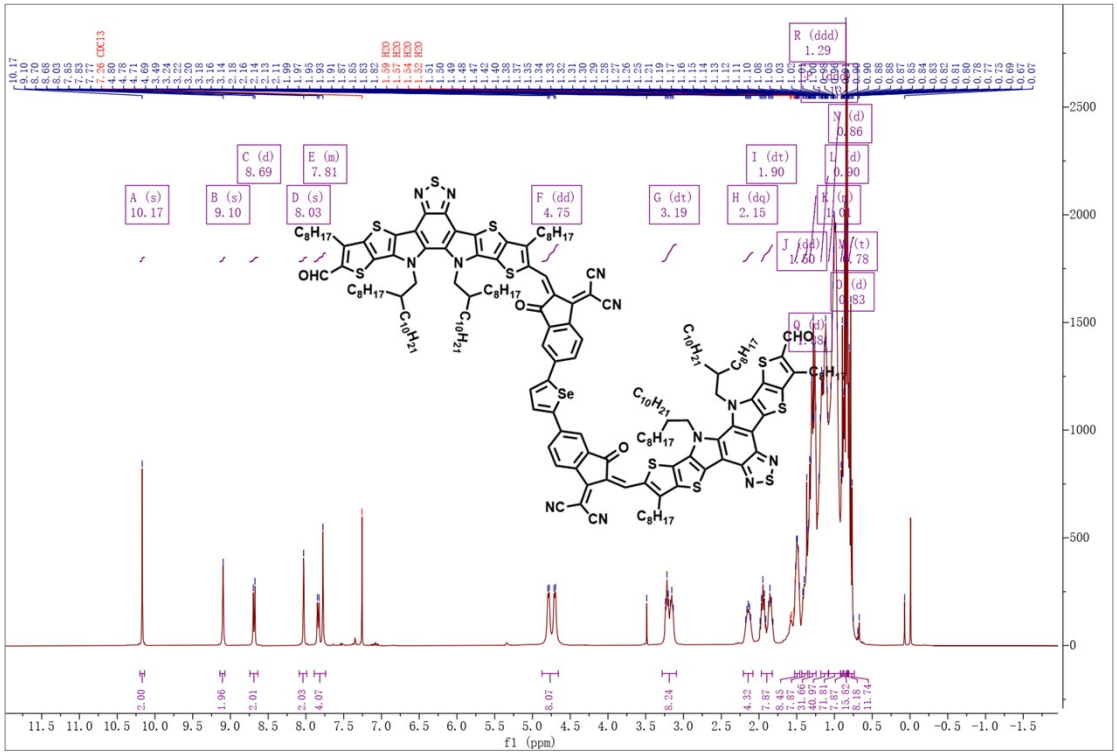

Figure S11. ^{1}H-NMR spectrum of compound **6 (X=S, Y=Se)**.

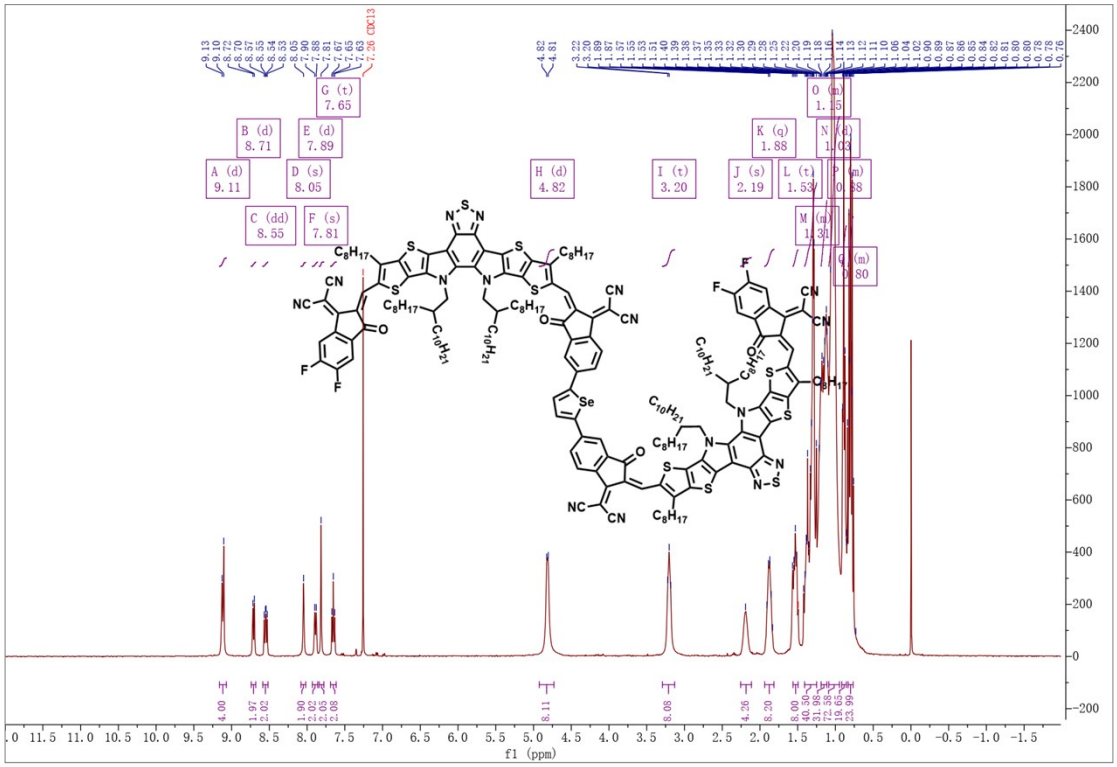

Figure S12. ^{1}H-NMR spectrum of compound **GMA-SSeS**.

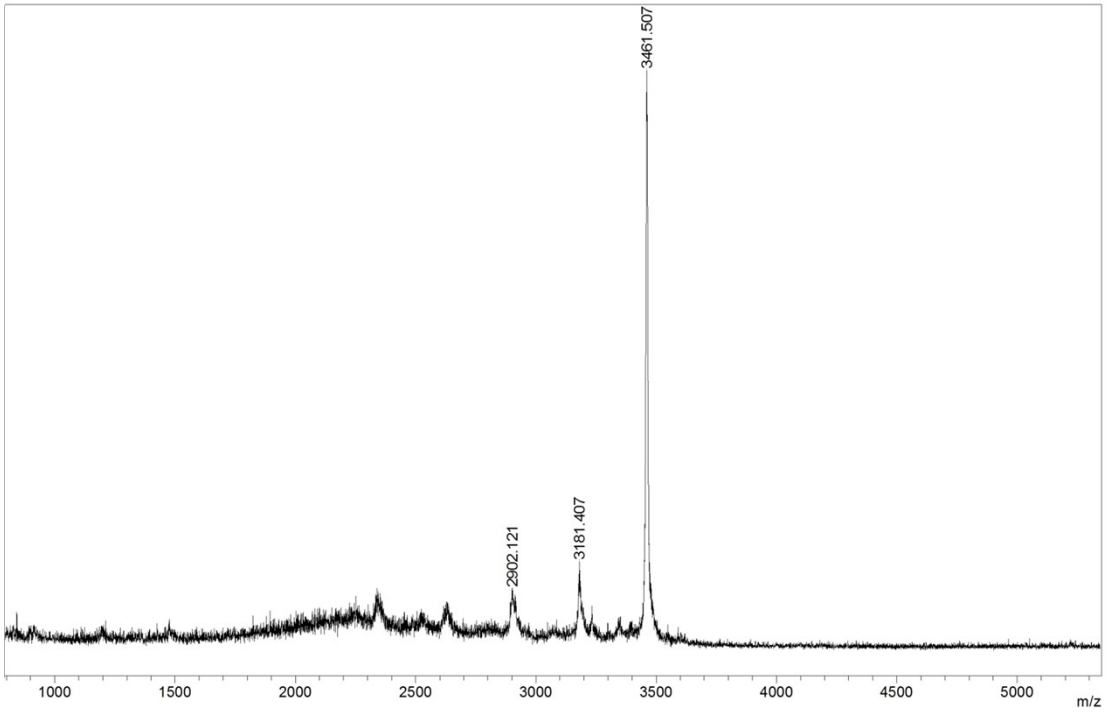

Figure S13. MALDI-TOF spectrum of **GMA-SSeS**.

Synthesis of compound 6 (X=Se, Y=S) and GMA-SeSSe, compound **5 (X=Se)** (0.46 g, 0.29 mmol), compound **e** (2,5-bis-trimethylstannyl- thiophene) (0.054 g, 0.13 mmol) and $Pd(PPh_3)_4$ (0.023 g, 0.02 mmol) were dissolved in toluene (20 ml) and stirred at 110 ℃ for 5 h under nitrogen atmosphere. The solvent was removed under vacuum after the reaction mixture was cooled to ambient temperature. Compound **6 (X=Se, Y=S)** were purified by chromatography in a silica gel column eluting with petroleum ether/dichloromethane (1/1.5, v/v), which yielding a blue solid as product **6 (X=Se, Y=S)** (0.25 g, 60% yield).

^{1}H NMR ($CDCl_3$): 10.06 (s, 2H), 9.27 (s, 2H), 8.75 (d, J=8.3 Hz, 2H), 8.12 (d, J=1.9 Hz, 2H), 7.97 (dd, J=8.3, 1.9 Hz, 2H), 7.62 (s, 2H), 4.67 (dd, J=25.6, 7.7 Hz, 8H), 3.28-3.14 (m, 8H), 2.12 (s, 4H), 1.97-1.84 (m, 8H), 1.60-1.46 (m, 24H), 1.36-1.23 (m, 36H), 1.17-1.03 (m, 48H), 1.02-0.83 (m, 84H), 0.78 (d, J=7.3 Hz, 12H).

Under nitrogen, compound **6 (X=Se, Y=S)** (0.25 g, 0.08 mmol), compound **f** 2-(5,6-difluoro-3-oxo-2,3-dihydro-1H-inden-1-ylidene) malononitrile (0.074 g, 0.32 mmol), BF_3OEt_2 (0.40 ml), acetic anhydride Ac_2O (0.50 ml) and toluene (10 ml) were added to a 25 ml round-bottled flask. After the reaction performed at 60 ℃ for 30 minutes, the mixture was poured into methanol and filtered. The residue was purified in a silica gel

column using petroleum ether/chloroform (1/3, v/v) as the eluent. Compound **GMA-SeSSe** was obtained as a dark blue solid (0.23 g, 80% yield).

^{1}H NMR ($CDCl_3$): 9.22 (d, J=15.7 Hz, 4H), 8.72 (d, J=8.2 Hz, 2H), 8.55 (dd, J=9.9, 6.4 Hz, 2H), 8.06 (s, 2H), 7.96 (d, J=8.2 Hz, 2H), 7.68-7.61 (m, 4H), 4.74 (s, 8H), 3.27 (s, 8H), 1.87 (s, 8H), 1.56 (s, 20H), 1.43-1.24 (m, 36H), 1.19-1.10 (m, 40H), 1.04 (s, 64H), 0.93-0.85 (m, 20H), 0.80 (p, J=7.2 Hz, 24H).

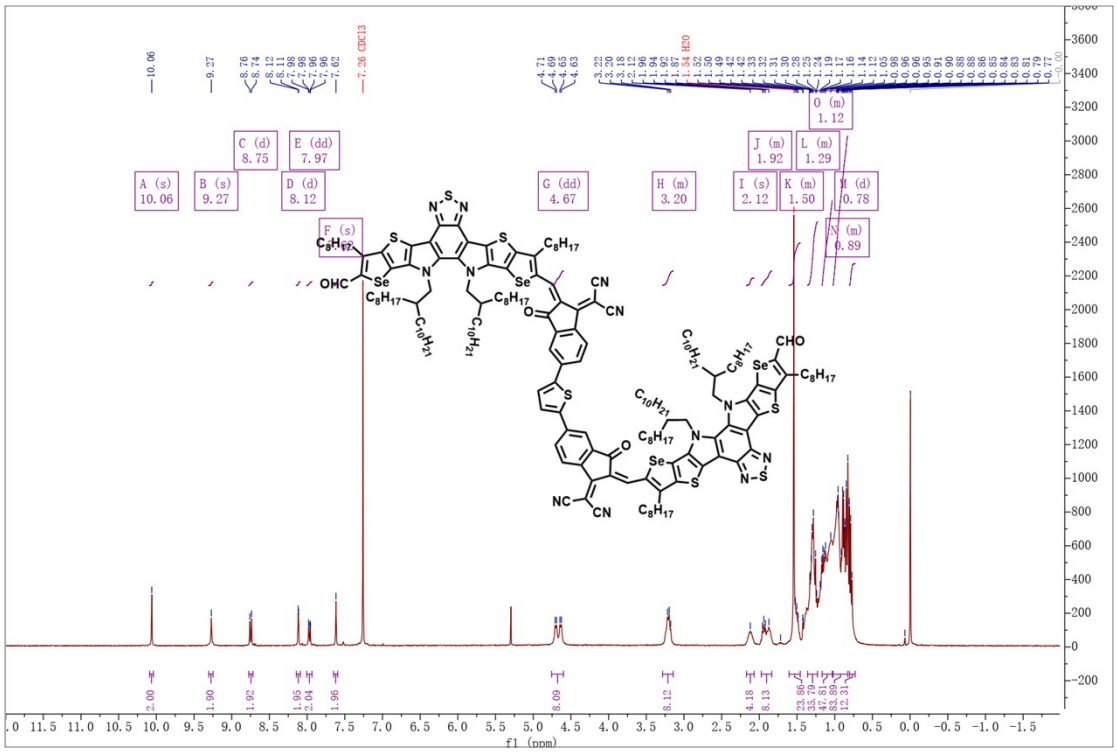

Figure S14. ^{1}H-NMR spectrum of compound **6 (X=Se, Y=S)**.

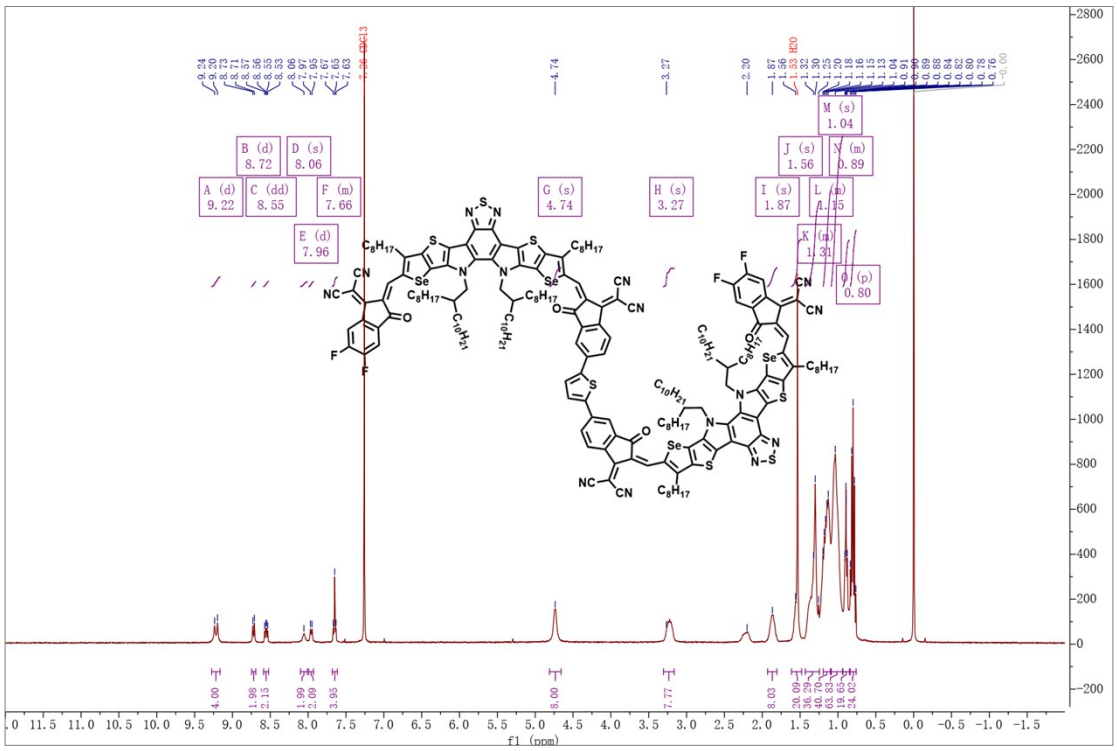

Figure S15. ^{1}H-NMR spectrum of compound **GMA-SeSSe**.

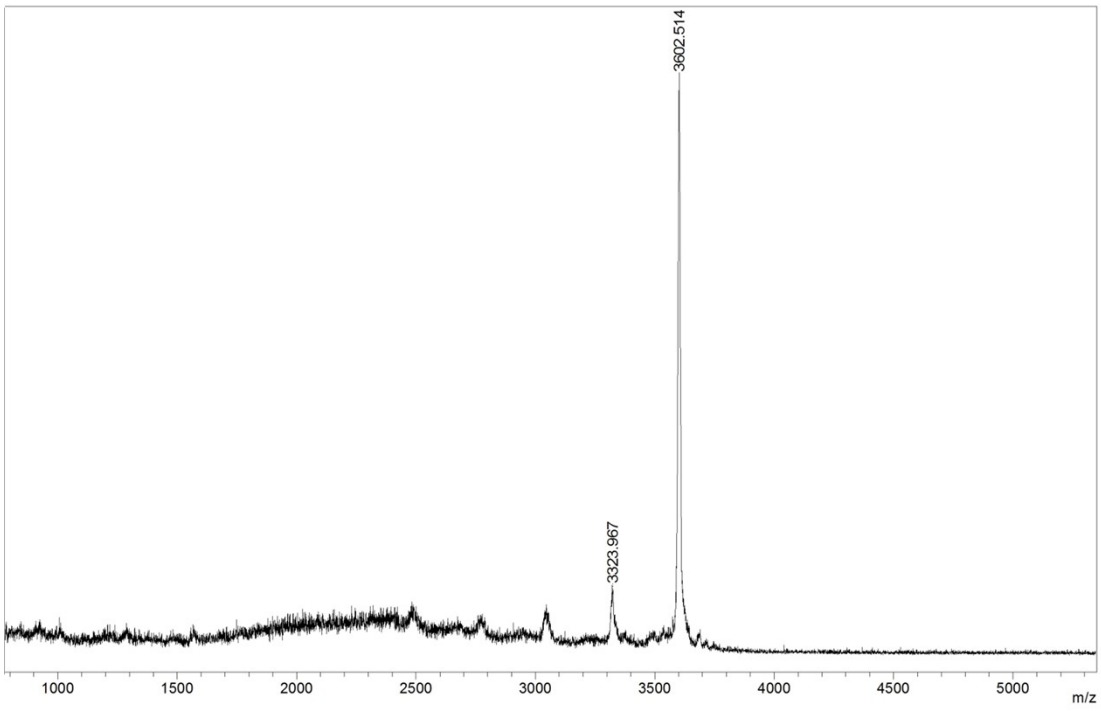

Figure S16. MALDI-TOF spectrum of **GMA-SeSSe**.

Synthesis of compound 6 (X=Se, Y=Se) and GMA-SeSeSe, compound **5 (X=Se)** (0.46 g, 0.29 mmol), compound **e** (2,5-bis-trimethylstannyl- selenophen) (0.059 g, 0.13 mmol) and $Pd(PPh_3)_4$ (0.023 g, 0.02 mmol) were dissolved in toluene (20 ml) and stirred at 110 ℃ for 5 h under nitrogen atmosphere. The solvent was removed under

vacuum after the reaction mixture was cooled to ambient temperature. Compound **6 (X=Se, Y=Se)** were purified by chromatography in a silica gel column eluting with petroleum ether/dichloromethane (1/2, v/v), which yielding a blue solid as product **6 (X=Se, Y=Se)** (0.21 g, 50% yield).

^{1}H NMR ($CDCl_3$): 10.08 (s, 2H), 9.19 (s, 2H), 8.68 (d, J=8.3 Hz, 2H), 7.99 (s, 2H), 7.84 (d, J=8.2 Hz, 2H), 7.75 (s, 2H), 4.80-4.58 (m, 8H), 3.28-3.06 (m, 8H), 2.15 (s, 4H), 1.95 (t, J=8.1 Hz, 4H), 1.83 (s, 4H), 1.31 (dd, J=33.2, 13.6 Hz, 76H), 1.13 (s, 36H), 0.98 (s, 32H), 0.84 (td, J = 17.4, 16.1, 8.9 Hz, 60H).

Under nitrogen, compound **6 (X=Se, Y=Se)** (0.21 g, 0.09 mmol), compound **f** 2-(5,6-difluoro-3-oxo-2,3-dihydro-1H-inden-1-ylidene) malononitrile (0.083 g, 0.36 mmol), BF_3OEt_2 (0.40 ml), acetic anhydride Ac_2O (0.50 ml) and toluene (10 ml) were added to a 25 ml round-bottled flask. After the reaction performed at 60 ℃ for 30 minutes, the mixture was poured into methanol and filtered. The residue was purified in a silica gel column using petroleum ether/chloroform (1/5, v/v) as the eluent. Compound **GMA-SeSeSe** was obtained as a dark blue solid (0.16 g, 50% yield).

^{1}H NMR ($CDCl_3$): 9.20 (d, J=10.1 Hz, 4H), 8.68 (d, J=8.0 Hz, 2H), 8.54 (dd, J=9.8, 6.4 Hz, 2H), 7.98 (s, 2H), 7.88 (d, J=8.5 Hz, 2H), 7.81 (s, 2H), 7.65 (t, J=7.5 Hz, 2H), 4.75 (s, 8H), 3.21 (d, J=9.8 Hz, 8H), 2.21 (s, 4H), 1.86 (q, J=8.3, 7.8 Hz, 8H), 1.58-1.22 (m, 76H), 1.09 (dq, J=24.0, 13.9, 12.7 Hz, 88H), 0.89 (t, J=6.4 Hz, 16H), 0.81 (q, J=6.6 Hz, 24H).

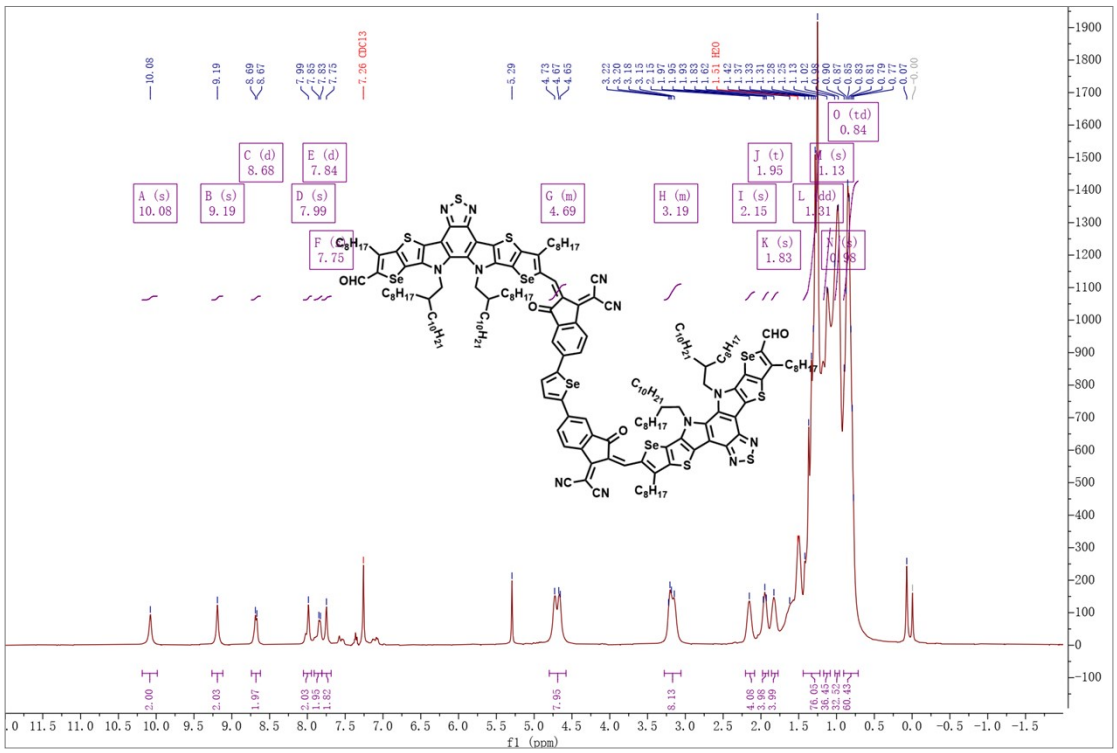

Figure S17. ^{1}H-NMR spectrum of compound **6 (X=Se, Y=Se)**.

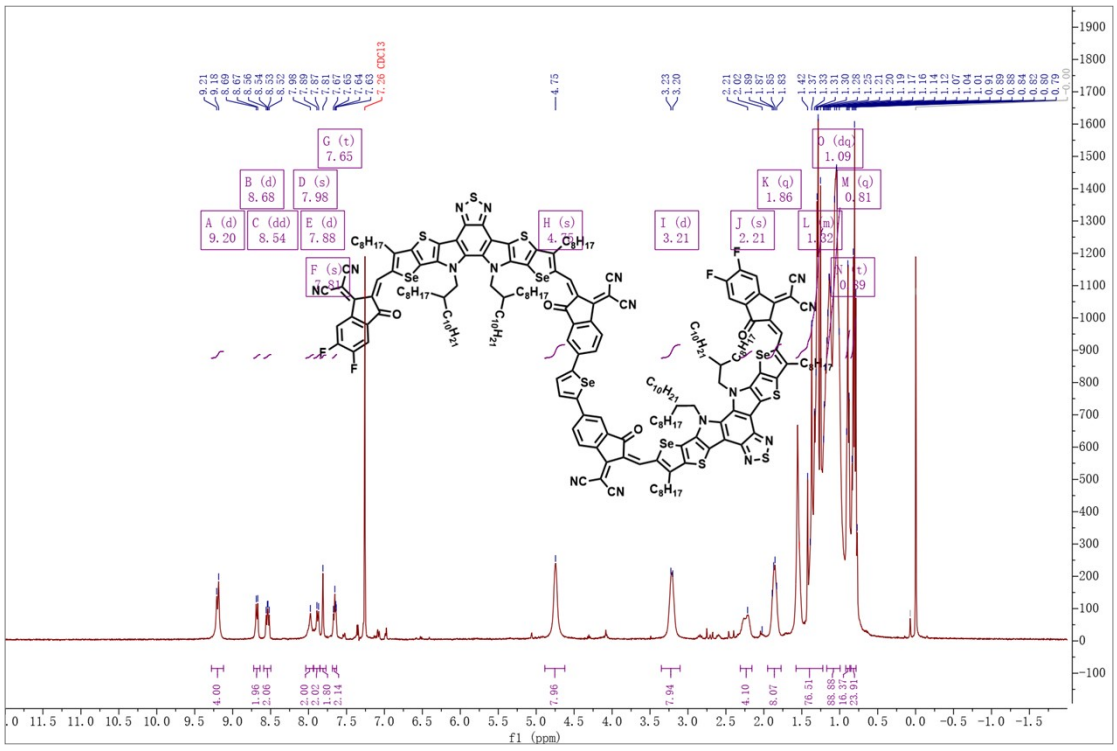

Figure S18. ^{1}H-NMR spectrum of compound **GMA-SeSeSe**.

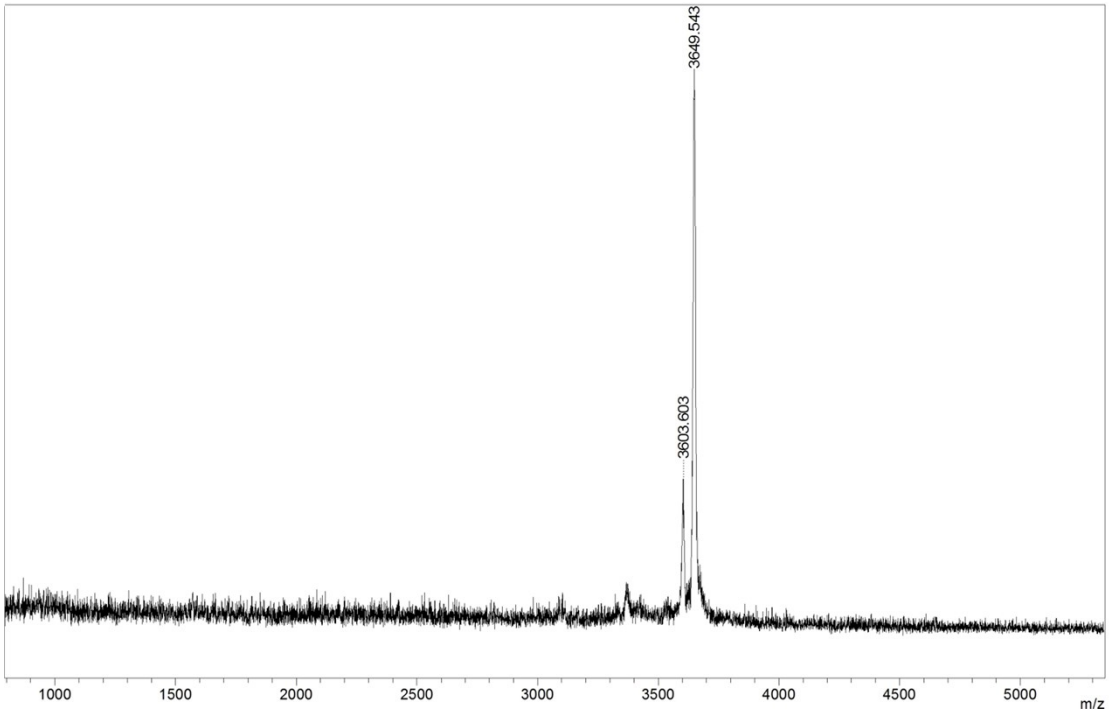

Figure S19. MALDI-TOF spectrum of **GMA-SeSeSe**.

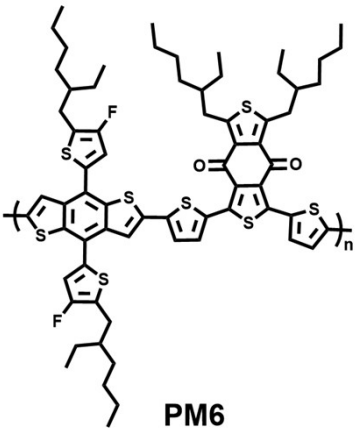

Figure S20. The chemical structure of **PM6**.

3. Measurements

Device fabrication and measurement

The OSCs were fabricated employing the conventional architecture of ITO/2PACz /PM6:GMAs/PDINN/Ag). The ITO glass was cleaned with deionized water, acetone and isopropanol in sequence, then treated with the UV-Ozone for 15 minutes. The 2PACz solution was spin-coated at 4000 rpm onto the ITO substrates for 30 seconds. The PM6 and GMAs were dissolved in solution with a ratio of 1:1 (w/w), the concentration of PM6 in CF solvent was 7 mg ml^{-1}, and the solution were stirred at

45˚C for 2h. Then the donor and GMAs were spin-coated with a speed of 3000 r min^{-1} on the 2PACz layer and treated with thermal annealing at 100˚C for 5 minutes. With the PDINN (1 mg ml^{-1}, 2000 r min^{-1}) spin-coated on the active layer, the devices were finally transferred to the evaporation tank to deposit 150 nm Ag. *J-V* measurements of devices were carried out in the Keithley 2440 source meter with a solar simulator (Newport-Oriel® Sol3A 450W) device. EQE measurements were conducted with the solar cell QE tester (QE-R, Enli Technology Co., Ltd).

Optical characterization and Estimation of glass-transition temperature:

UV-Vis-NIR absorption spectra were acquired on a Perkin-Elmer Lambda 950 spectrophotometer.

Photoluminescence spectra were acquired on a HORIBA FL3-111 spectrophotometer.

The glass transition temperature (T_g) of GMA corresponds to an onset temperature at which the GMA becomes mobile to reorganize the imperfect GMAs crystals. UV-vis spectroscopy was used to determine T_gs of the GMAs. The absorption spectra of GMAs films were measured with increasing thermal annealing temperatures from room temperature to 240 °C. Then, a deviation metric (DM_T) was calculated by quantifying the change in the absorbance of each film during annealing, following the method from Samuel E. Root et al.[1]

$$DM_T = \sum_{\lambda_{min}}^{\lambda_{max}} \left[I_{RT}(\lambda) - I_T(\lambda)\right]^2$$

where λ is the wavelength, λ_{max} and λ_{min} are the upper and lower bounds of the optical sweep, respectively. $I_{RT}(\lambda)$ and $I_T(\lambda)$ are the normalized absorption intensities of the as-cast (room temperature) and annealed films, respectively. Then, T_gs were determined to points where the two interpolated lines in low- and high-temperature regions intersect.

Estimation of diffusion coefficient at 85°C (D_{85}):

The D_{85}s of the GMAs (in blend films with PM6) were estimated following the method (*i.e.*, Ghasemi−O'Connor−Ade framework) in previous literature.[2] In the study, Ghasemi *et al*. estimated T_gs (or coldcrystallization temperatures, T_{cc}s) of various

acceptor constituents (*i.e.*, EH-IDTBR, di-PDI, IT-M, IEICO-Cl, ITIC-4Cl, and Y6) by measuring DM_T of UV-absorbances or DSC of pristine acceptor materials. They also monitored D_{85}s of the acceptor constituents in blend films with specific donors (i.e., P3HT, FTAZ/HTAZ, PTB7-Th, and PBDB-T/PBDB-T2F (PM6)) at 85°C by obtaining time-of-flight secondary ion mass spectrometry (ToF-SIMS) profiles. They found that D_{85}s of the acceptors (in the blend films with given donors) had strong correlation with their T_gs, showing an exponential decrease in the D_{85} as the T_g increased ($D_{85}(cm^2\ s^{-1}) = a \times e^{b \times Tg(K)}$); the coefficients (a and b) in the exponential equations were determined depending on the given donors. When PM6 or PBDB-T donor was used, the D_{85}s of the acceptor components in the blend with donors were determined as $D_{85}(cm^2\ s^{-1}) = 1.2 \times 10^7 \times e^{-0.15 \times Tg\ (K)}$.

Therefore, in this study, we estimated the D_{85}s of four GMAs in their blends with donor PM6 by using the same correlation of $D_{85}(cm^2 s^{-1}) = 1.2 \times 10^7 \times e^{-0.15 \times Tg\ (K)}$. And, the T_gs were measured from the DM_T of film UV–Vis absorbances (T_g of GMA-SSS = 471.15 K, T_g of GMA-SSeS = 461.15 K, T_g of GMA-SeSSe = 463.15 K, and T_g of GMA-SeSeSe = 425.15 K). We obtained the D_{85} of GMA-SSS = 2.44×10^{-24} $cm^2\ s^{-1}$, D_{85} of GMA-SSeS = 1.09×10^{-23} $cm^2\ s^{-1}$, D_{85} of GMA-SeSSe = 8.08×10^{-24} $cm^2\ s^{-1}$ and D_{85} of GMA-SeSeSe = 4.21×10^{-23} $cm^2\ s^{-1}$.

Cyclic Voltammetry (CV)

The energy levels for PM6, GMA-SSS, GMA-SSeS, GMA-SeSSe and GMA-SeSeSe were measured by cyclic voltammetry (CV), which was performed by using Ag/AgCl as reference electrode in $C_{16}H_{36}NPF_6$ solution, and ferrocene/ferrocenium (Fc/Fc^+) (-0.1 eV versus Ag/AgCl) was used as internal reference. The HOMO and LUMO were calculated according to the following equation:

$$E_{HOMO/LUMO} = -(\varphi_{ox/red} - \varphi_{Fc/Fc^+} + 4.8)\ eV$$

Where φ_{OX} is the onset of oxidation and the φ_{red} relates to the reduction potential, respectively.

Space charge limited current (SCLC) method

Electron-only devices were fabricated using the structure of ITO/Al/active layers/PDINN/Ag. Firstly, after being cleaned with deionized water, acetone and

isopropanol, the all-ITO glass was deposited with 100 nm Al and then the blends of PM6 and GMAs were spin-coated on the Al layer and treated with 95 ℃ for 5 minutes. With the PDINN spin-coated on the active layer, the devices were finally transferred to the evaporation tank to deposit 150 nm Ag.

Hole-only devices were fabricated with the structure of ITO/2PACz/active layers/MoO_3/Ag. After being cleaned with deionized water, acetone and isopropanol, the all-ITO glass was treated with the UV-Ozone for 15 minutes. The 2PACz solution was spin-coated at 4000 rpm onto the ITO substrates for 30 seconds. Then the blends of PM6 and GMAs were spin-coated on the 2PACz layer and treated with 95℃ for 5 minutes. Then devices were finally transferred to the evaporation tank to deposit 10 nm MoO_3 and then 150 nm Ag.

The mobilities were obtained by taking current-voltage curves and fitting the results to a space charge limited form, where the SCLC is described by:

$$J = \frac{9\varepsilon_0\varepsilon_R\mu V^2}{8L^3}$$

Where ε_0 is the permittivity of free space, ε_R is the relative permittivity of the material (assumed to be 3), μ is the electron or hole mobility and L is the thickness of the film. From the plots of $J^{1/2}$ vs V, electron or hole mobilities can be deduced.

Morphology Characterization

AFM height and phase images were measured by Bruker Dimension ICON to explore the characteristic of morphology. TEM was performed on a JEOL 2100 (JEOL., Ltd). The samples were fabricated in accordance with the conditions of the best devices. GIWAXS was measured by Xeuss 3.0 UHR.

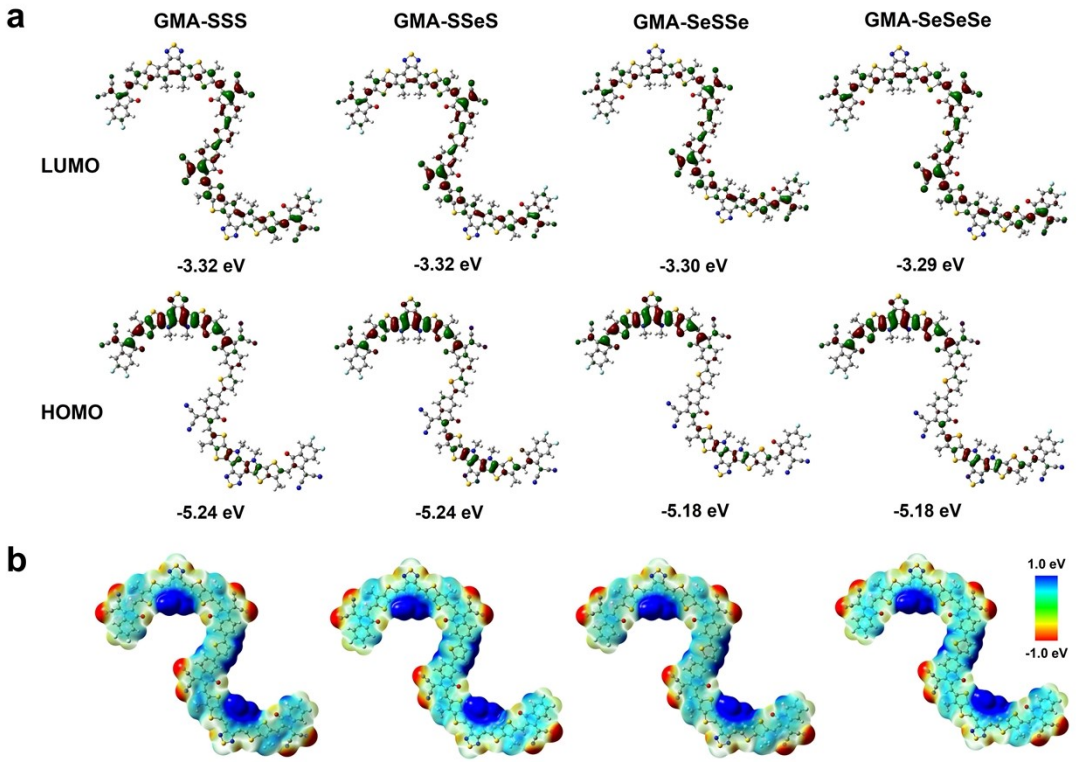

Figure S21. (a) The LUMO and HOMO orbitals of GMA-SSS, GMA-SSeS, GMA-SeSSe and GMA-SeSeSe computed with B3LYP/6-31G, and the Eg values are calculated to be 1.92, 1.92, 1.88 and 1.89 eV, respectively. (b) Map of the electrostatic potential (ESP) surfaces calculated by DFT, where red color indicates greater negative charge and blue color indicates greater positive charge. Most molecular surfaces of four GMAs exhibited positive ESPs, indicating their electron-accepting nature, which are very different with the donor PM6, suggesting good compatibility.

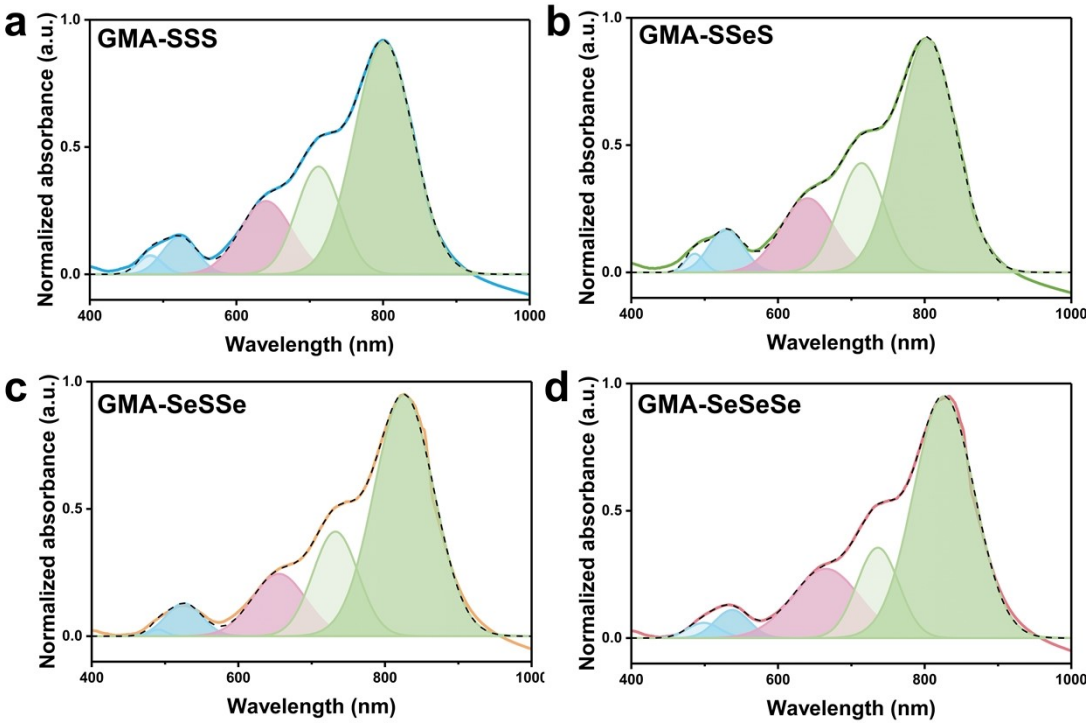

Figure S22. Absorption peaks fitting profiles of (a) GMA-SSS, (b) GMA-SSeS, (c) GMA-SeSSe and (d) GMA-SeSeSe neat films. The peaks at ~800 nm (GMA-SSS and GMA-SSeS), ~830 nm (GMA-SeSSe and GMA-SeSeSe) and ~710 nm (GMA-SSS and GMA-SSeS), ~730 nm (GMA-SeSSe and GMA-SeSeSe) are assigned to the S0→S1 electronic transition with partial charge transfer (CT) character and its first vibronic (0-1) side band, respectively (green shaded band). The blue shifted bands at ~640 nm (GMA-SSS and GMA-SSeS) and ~660 nm (GMA-SeSSe and GMA-SeSeSe) belong to separate, weakly allowed S0→S1 electronic transition due to the presence of amorphous phase (red shaded band). The broad band around 520 nm of four GMAs is associated with π-π* electronic transition (blue shaded band).

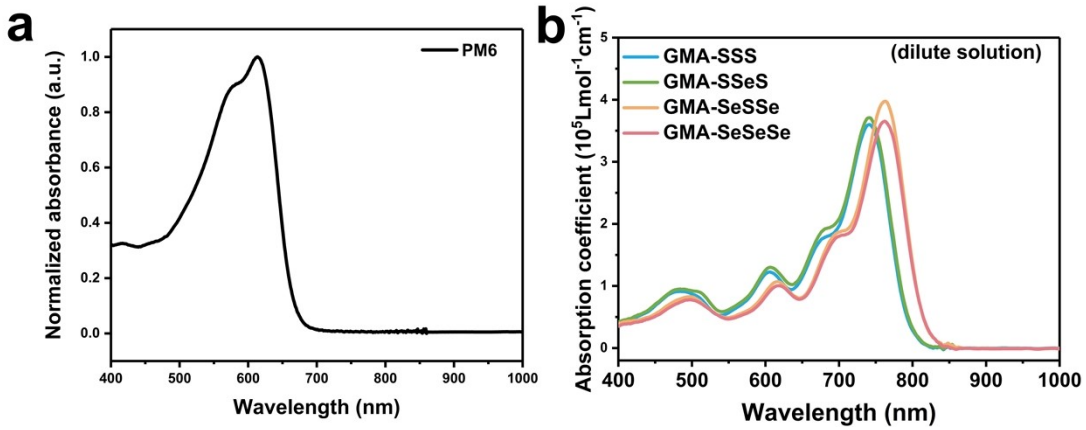

Figure S23. (a) Normalized absorption profile of neat PM6 film. (b) Absorption spectra of four GMAs in dilute chloroform solutions, and calculated molar absorption coefficient values of GMA-SSS, GMA-SSeS, GMA-SeSSe and GMA-SeSeSe are 3.60, 3.71, 3.97 and 3.65×10^5 L mol^{-1} cm^{-1}, respectively.

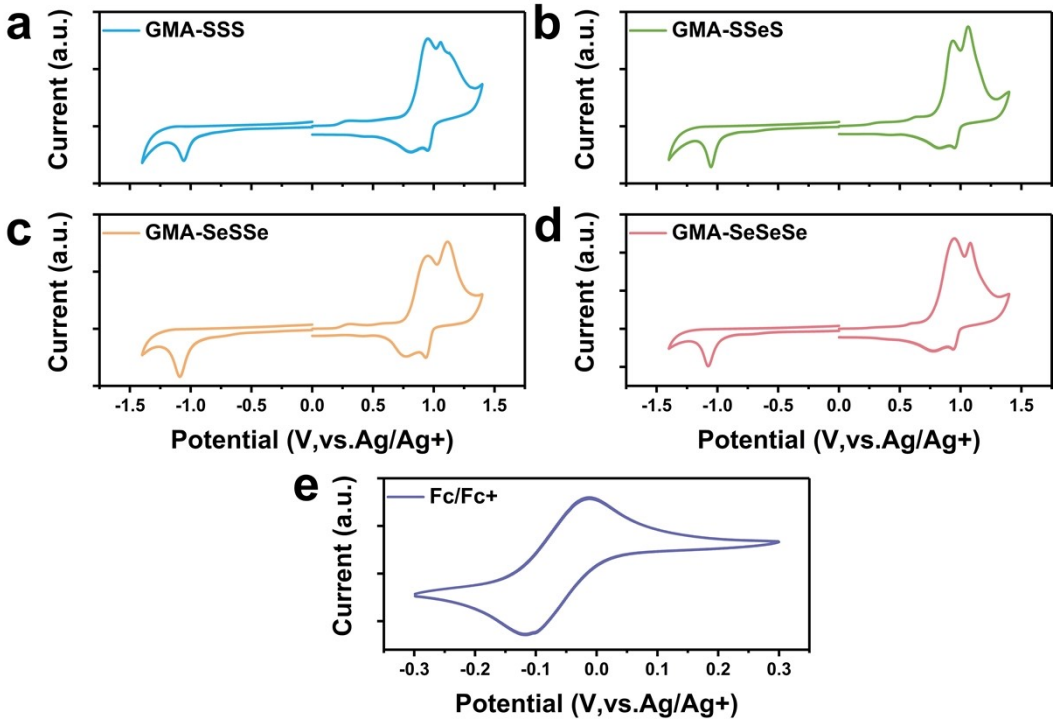

Figure S24. Cyclic voltammograms curves of (a) GMA-SSS, (b) GMA-SSeS, (c) GMA-SeSSe, (d) GMA-SeSeSe and (e) ferrocene/ferrocenium.

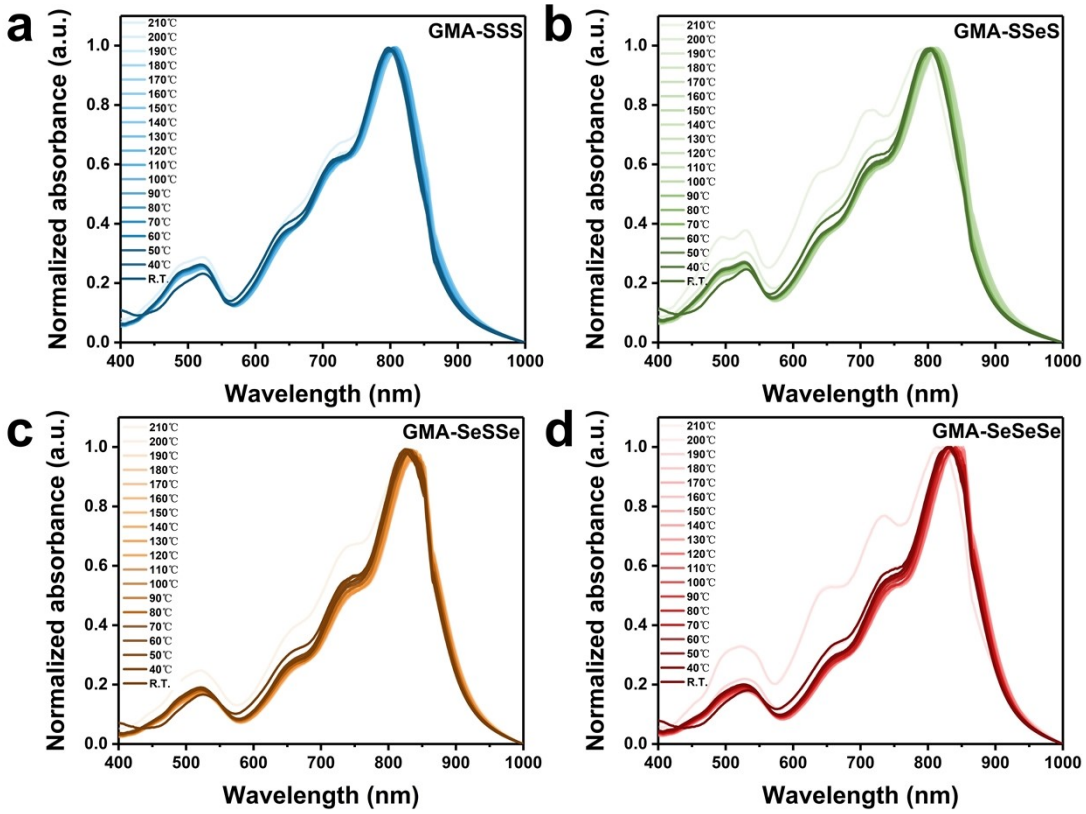

Figure S25. UV-Vis absorption spectra of (a) GMA-SSS, (b) GMA-SSeS, (c) GMA-SeSSe and (d) GMA-SeSeSe with increasing thermal annealing temperatures from room temperature (R.T.) to 210 °C.

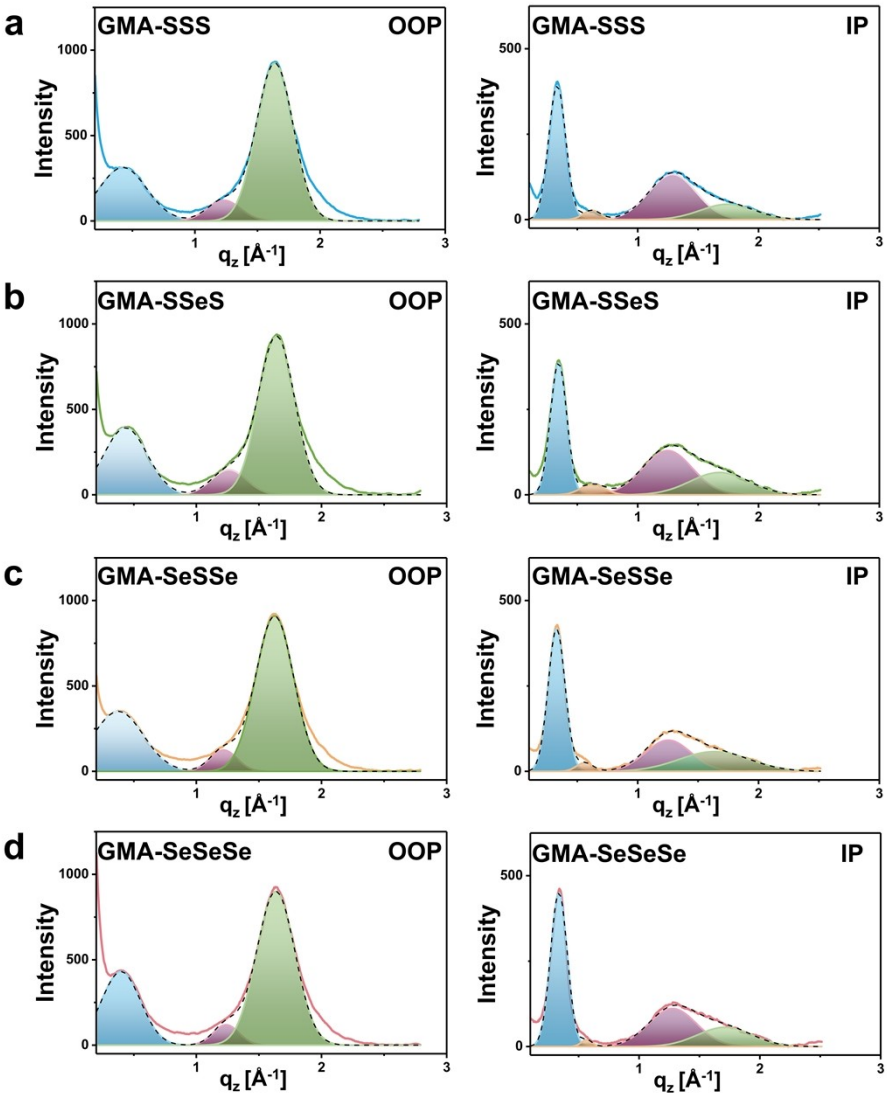

Figure S26. Peak fitting analysis of OOP and IP extracted line-cut profiles of the 2D GIWAXS patterns of four GMAs: (a) GMA-SSS, (b) GMA-SSeS, (c) GMA-SeSSe and (d) GMA-SeSeSe. Along the OOP direction, all neat GMAs films show lamellar stacking (100) and (300) diffraction peaks (blue and red shaded band, respectively), and pronounced π-π stacking (010) diffraction peaks (green shaded band). Along the IP direction, all neat GMAs films show pronounced lamellar stacking (100), (200) and (400) diffraction peaks (blue, yellow and red shaded band, respectively), and π-π stacking (010) diffraction peaks (green shaded band).

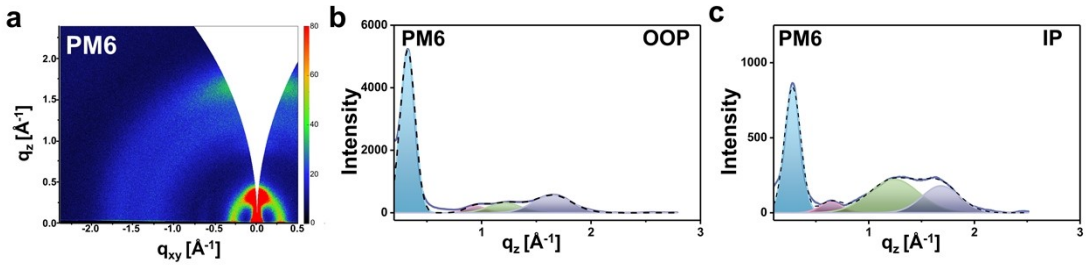

Figure S27. (a) 2D GIWAXS patterns, peak fitting analysis of (b) OOP and (c) IP extracted line-cut profiles of PM6. Along the OOP direction, neat PM6 film shows pronounced lamellar stacking (100), (300) and (400) diffraction peaks (blue, red and green shaded band, respectively), and π-π

stacking (010) diffraction peaks (purple shaded band). Along the IP direction, neat PM6 film shows pronounced lamellar stacking (100), (200) and (400) diffraction peaks (blue, red and green shaded band, respectively), and π-π stacking (010) diffraction peaks (purple shaded band).

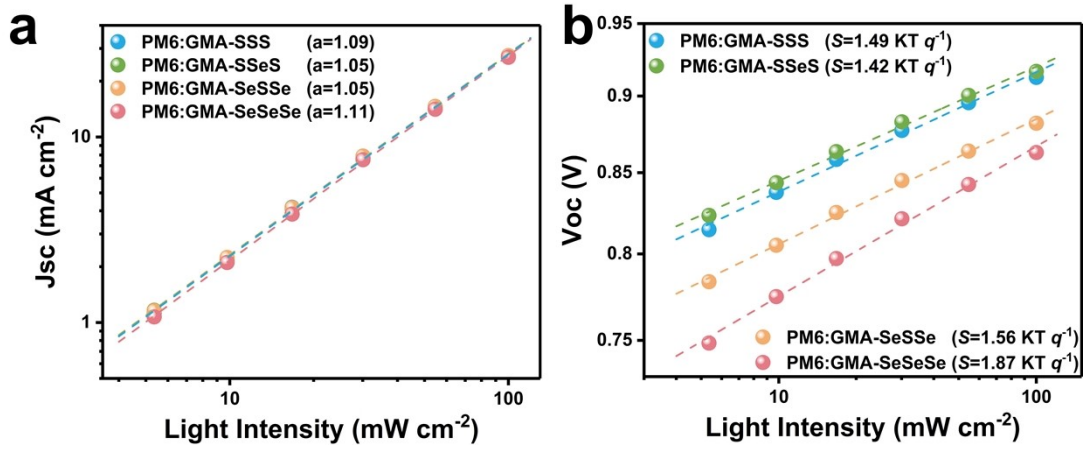

Figure S28. Light-intensity-dependent (a) J_{SC} and (b) V_{OC} plots of four PM6:GMAs-based devices.

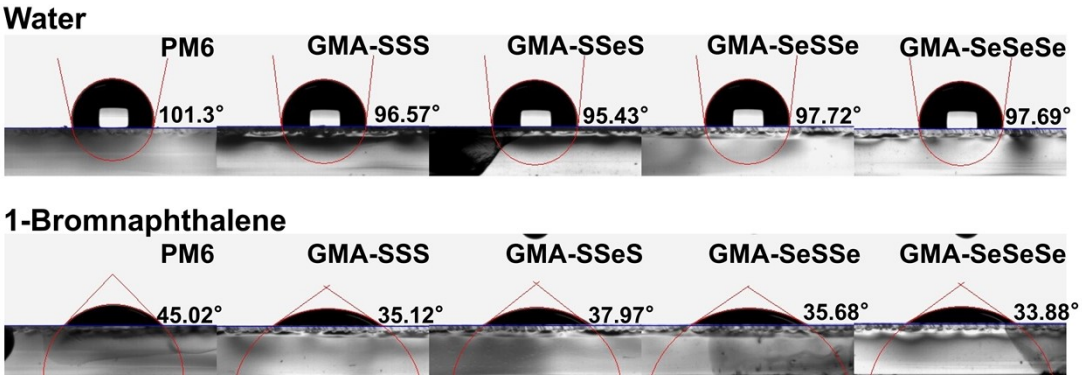

Figure S29. The contact angles of water and 1-Bromnaphthalene on the pristine films.

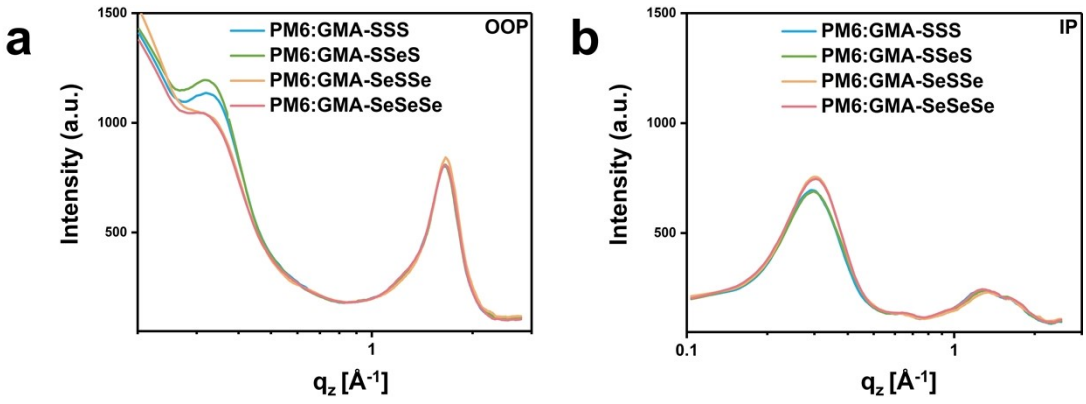

Figure S30. (a) OOP and (b) IP extracted line-cut profiles of the 2D GIWAXS patterns of four PM6:GMAs-based blends.

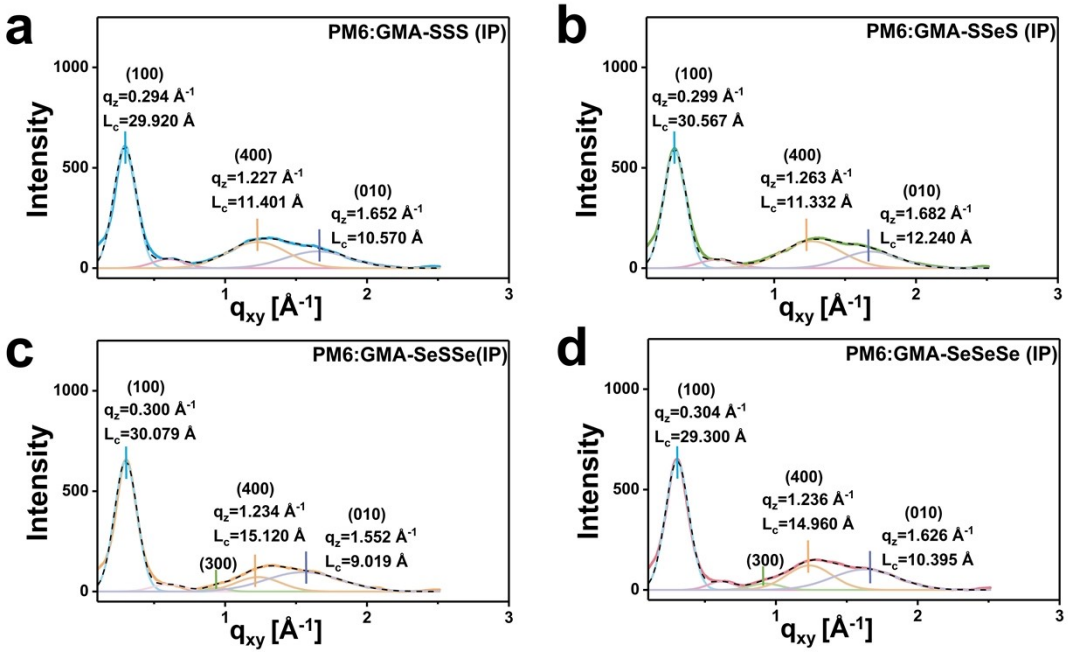

Figure S31. Peak fitting analysis of IP extracted line-cut profiles of the 2D GIWAXS patterns of four PM6:GMAs-based blends.

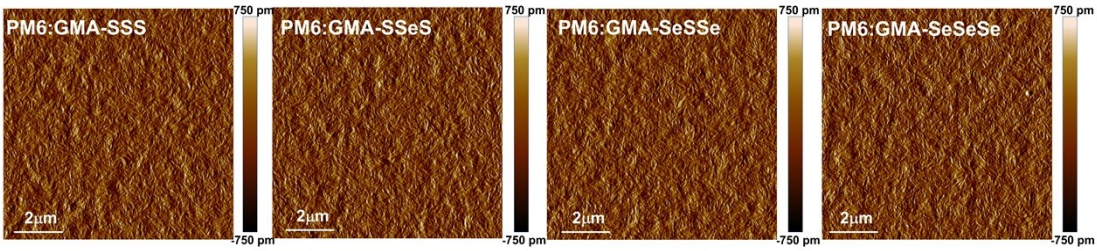

Figure S32. AFM phase images of four PM6:GMAs-based blends.

Table S1. GIWAXS characteristics of the neat PM6, GMA-SSS, GMA-SSeS, GMA-SeSSe and GMA-SeSeSe films.

		q (Å^{-1})	d (Å)[a]	FWHM (Å^{-1})	L_c (Å)[b]
PM6	OOP (100)	0.324	19.393	0.161	35.123
	OOP (300)	0.948	6.628	0.221	25.588
	OOP (400)	1.211	5.188	0.347	16.296
	OOP (010)	1.648	3.813	0.412	13.725
	IP (100)	0.279	22.520	0.179	31.591
	IP (200)	0.641	9.802	0.249	22.710
	IP (400)	1.238	5.075	0.552	10.244

	IP (010)	1.682	3.736	0.421	13.432
GMA-SSS	OOP (100)	0.423	14.854	0.449	12.594
	OOP (300)	1.231	5.104	0.314	18.009
	OOP (010)	1.639	3.834	0.345	16.391
	IP (100)	0.333	18.868	0.168	33.660
	IP (200)	0.620	10.134	0.170	33.264
	IP (400)	1.287	4.882	0.462	12.240
	IP (010)	1.742	3.607	0.528	10.710
GMA-SSeS	OOP (100)	0.434	14.477	0.408	13.860
	OOP (300)	1.260	4.987	0.329	17.188
	OOP (010)	1.641	3.829	0.340	16.632
	IP (100)	0.344	18.265	0.158	35.790
	IP (200)	0.627	10.021	0.234	24.166
	IP (400)	1.246	5.043	0.483	11.708
	IP (010)	1.676	3.749	0.570	9.921
GMA-SeSSe	OOP (100)	0.376	16.711	0.470	12.032
	OOP (300)	1.216	5.167	0.255	22.176
	OOP (010)	1.625	3.867	0.359	15.752
	IP (100)	0.328	19.156	0.165	34.272
	IP (200)	0.561	11.200	0.164	34.481
	IP (400)	1.252	5.019	0.442	12.794
	IP (010)	1.633	3.848	0.686	8.243
GMA-SeSeSe	OOP (100)	0.397	15.827	0.366	15.450
	OOP (300)	1.237	5.079	0.243	23.271
	OOP (010)	1.635	3.843	0.360	15.708
	IP (100)	0.336	18.700	0.163	34.692
	IP (200)	0.566	11.101	0.108	52.360
	IP (400)	1.277	4.920	0.466	12.135
	IP (010)	1.710	3.674	0.532	10.629

[a] The d-spacing estimated from the equation d=2π/q.

[b] The Coherent length estimated from the Scherrer's equation L_c= 2πk/FWHM, where k is a shape factor (here use 0.9).

Table S2. Detailed photovoltaic parameters of the PM6:GMA-SSS, PM6:GMA-SSeS, PM6:GMA-SeSSe and PM6:GMA-SeSeSe based devices by optimal conditions under illumination of AM 1.5 G, 100 mW cm^{-2}.[a]

	V_{OC} [V]	J_{SC} [mA cm^{-2}]	FF [%]	PCE [%]
PM6:GMA-SSS	0.910	27.05	75.47	18.58
	0.913	27.13	75.35	18.66
	0.914	27.08	75.25	18.63
	0.913	27.12	75.17	18.61
	0.912	27.10	75.01	18.54
	0.911	27.05	75.07	18.51
	0.911	27.06	75.02	18.49
	0.910	26.98	75.20	18.46
	0.910	27.01	74.95	18.42
	0.909	27.01	74.90	18.39
	0.909	26.98	74.92	18.37
	0.915	26.65	76.10	18.55
	0.913	26.62	76.05	18.49
	0.912	26.56	75.91	18.38
	0.911	26.79	75.62	18.45
	0.910	26.75	75.57	18.40
Average[b]	**0.911**	**26.93**	**75.36**	**18.50**

	V_{OC} [V]	J_{SC} [mA cm^{-2}]	FF [%]	PCE [%]
PM6:GMA-SSeS	0.917	27.38	77.12	19.37
	0.917	27.35	77.04	19.32
	0.917	27.36	76.98	19.30
	0.915	27.34	76.96	19.26
	0.914	27.36	77.01	19.26
	0.914	27.32	76.99	19.22
	0.913	27.35	76.82	19.19
	0.913	27.34	76.87	19.19
	0.918	27.40	76.88	19.33
	0.917	27.44	76.83	19.34
	0.917	27.41	76.73	19.28
	0.916	27.43	76.76	19.29
	0.916	27.32	76.80	19.21
	0.920	27.23	77.03	19.30
	0.919	27.16	76.99	19.21
	0.917	27.17	76.88	19.17

Average[b]	**0.916**	**27.34**	**76.92**	**19.26**

	V_{OC} [V]	J_{SC} [mA cm^{-2}]	FF [%]	PCE [%]
PM6:GMA-SeSSe	0.878	27.46	74.36	17.92
	0.877	27.46	74.07	17.83
	0.880	27.33	75.10	18.06
	0.879	27.37	74.61	17.95
	0.880	27.95	73.25	18.02
	0.881	27.99	73.34	18.09
	0.880	27.93	73.43	18.05
	0.879	27.95	73.05	17.95
	0.877	27.99	73.11	17.96
	0.882	27.47	74.99	18.17
	0.881	27.48	74.79	18.11
	0.880	27.49	74.72	18.08
	0.879	27.44	74.88	18.07
	0.879	27.48	74.72	18.04
	0.878	27.44	74.71	18.01
	0.878	27.48	74.61	18.00
Average[b]	**0.882**	**27.61**	**74.23**	**18.02**

	V_{OC} [V]	J_{SC} [mA cm^{-2}]	FF [%]	PCE [%]
PM6:GMA-SeSeSe	0.868	26.30	71.60	16.34
	0.866	26.32	71.49	16.30
	0.865	26.29	71.68	16.31
	0.864	26.88	70.97	16.48
	0.863	26.88	71.04	16.48
	0.862	26.90	70.63	16.39
	0.863	26.90	70.75	16.42
	0.865	26.91	70.83	16.49
	0.864	26.85	70.53	16.36
	0.863	26.90	70.50	16.37
	0.863	26.86	70.70	16.38
	0.862	26.84	70.40	16.29
	0.866	26.83	70.52	16.38
	0.864	26.78	70.56	16.32
	0.863	26.77	70.53	16.29
	0.863	26.81	70.31	16.27
Average[b]	**0.864**	**26.75**	**70.83**	**16.37**

[a]The device architecture is ITO/2PACz/ PM6:GMAs (1:1) /PDINN/Ag, PM6 is 7 mg/mL in chloroform with 0.75 vol% CN, the resulting solutions are spin-casted at 3000 rpm onto the 2PACz layer, TA (95 ℃ for 10 min).

[b] The average values are obtained from 16 independent devices.

Table S3. Photovoltaic parameters of PM6:GMAs-based OSCs under AM 1.5G irradiation (100 mW cm^{-2}) when employing PEDOT:PSS as hole transport layer.

GMAs	V_{OC} [V]	J_{SC} [mA cm^{-2}]	FF [%]	PCE [%]
GMA-SSS	0.911	26.07	74.74	17.76
GMA-SSeS	0.912	26.86	76.06	18.64
GMA-SeSSe	0.876	27.27	72.29	17.28
GMA-SeSeSe	0.865	25.38	71.68	15.74

Table S4. Detailed photovoltaic parameters of GMAs-based binary BHJ OSCs reported in recent years.

Acceptor	**Donor**	**V_{OC} [V]**	**J_{SC} [mA cm^{-2}]**	**FF [%]**	**PCE [%]**	**Energy Loss [eV]**	**Device stability (Stability condition)**	**Ref.**
OY2	PBDB-T	0.837	24.37	71.79	14.69			[3]
OY3		0.839	23.76	74.58	14.87		$t_{80\%}$~25000 h (1sun)	
OY4		0.814	24.39	74.69	14.82			
QM1	PM6	0.91	25.23	74.01	17.05	0.54	$t_{90\%}$~1400 h (1 sun)	[4]
QM2		0.91	25.42	70.50	16.36	0.53		
*d*BTICγ-EH	PM6	0.92	21.43	73.28	14.48		$t_{80\%}$~1020 h (1 sun)	[5]
*d*BTICγ-BO		0.91	20.97	70.26	13.42		$t_{80\%}$~840 h (1 sun)	
*t*BTICγ-EH		0.90	21.25	68.76	13.16		$t_{80\%}$~840 h (1 sun)	
2BTP-2F-T	PM6	0.911	25.50	78.28	18.19	0.52	$t_{80\%}$~443 h (1 sun)	[6]
TDY-α	PM6	0.864	26.9	78.0	18.1		$t_{80\%}$~34747 h (1 sun)	[7]
TDY-β		0.849	26.1	76.6	17.0		$t_{80\%}$~31000 h (1 sun)	
CH8-0	PM6	0.936	22.61	72.1	15.26	0.490	$t_{78\%}$~360 h (65 ℃)	[8]
CH8-1		0.923	24.89	74.2	17.05	0.518	$t_{85\%}$~200 h (1 sun)	
CH8-2		0.928	24.24	74.9	16.84	0.529	$t_{85\%}$~360 h (65 ℃)	
CH8-3	PM6	0.915	24.44	77.0	17.22	0.529	$t_{80\%}$~250 h (65 ℃)	[9]
CH8-4		0.894	26.05	75.5	17.58	0.515	$t_{80\%}$~250 h (65 ℃)	
CH8-5		0.902	24.75	75.2	16.79	0.520	$t_{80\%}$~250 h (65 ℃)	
DYV	PM6	0.910	25.972	76.215	18.013		$t_{80\%}$~700 h (1 sun)	[10]
DYVC		0.915	24.874	73.857	16.809			
DYTVT		0.935	22.903	68.145	14.593			

DYB		0.939	20.509	67.415	12.983			
DYID		0.913	12.901	46.995	5.534			
DITV		0.937	20.394	72.571	13.643			
DITID		0.935	13.927	52.458	6.831			
DYC6		0.936	18.751	67.724	11.838			
DYC8		0.947	20.467	68.449	13.267			
DYC10		0.947	22.277	68.656	14.484		$t_{77\%}$~700 h (1 sun)	
DYSe-I	PM6	0.94	23.5	74.00	16.8		$t_{80\%}$~514 h (100 ℃)	[11]
DYSe-O		0.95	19.7	79.00	14.0		$t_{80\%}$~115 h (100 ℃)	
DYT	PM6	0.94	24.08	76.00	17.30		$t_{80\%}$~2493 h (1 sun)	[12]
DYV		0.93	25.64	78.00	18.60		$t_{80\%}$~4005 h (1 sun)	
DYTVT		0.95	24.82	74.00	17.68		$t_{80\%}$~5419 h (1 sun)	
DYT	PM6	0.942	24.89	74.00	17.29	0.503	$t_{80\%}$~2551 h (1 sun)	[13]
TYT		0.964	25.07	75.00	18.15	0.492	$t_{80\%}$~8454 h (1 sun)	
DY1	PM6	0.87	25.67	73.24	16.46			[14]
DY2		0.87	26.60	76.85	17.85	0.580	$t_{83\%}$~700 h (1 sun)	
DY3		0.87	26.20	76.21	17.33			
CH-D1	PM6	0.949	23.90	73.20	16.62			[15]
DYBO	PM6	0.968	24.623	75.800	18.082	0.484	$t_{80\%}$~6085 h (1 sun)	[16]
DYA-I	D18	0.938	25.67	78.00	18.83		$t_{80\%}$~5380 h (1 sun)	[17]
DYA-IO		0.948	24.29	76.00	17.54		$t_{80\%}$~4255 h (1 sun)	
DYA-O		0.961	23.32	73.00	16.45		$t_{80\%}$~3337 h (1 sun)	
dBTIC-δV-BO	PBQx-H-TF	0.96	20.67	66.06	13.15	0.578	$t_{80\%}$~750 h (1 sun)	[18]
dBTIC-γV-BO		0.91	24.52	76.58	17.14	0.557	$t_{80\%}$~2150 h (1 sun)	
dBTIC-γV-OD-2Cl		0.87	24.65	74.71	16.04	0.566	$t_{80\%}$~1100 h (1 sun)	
G-Dimer	PM6	0.904	24.39	78.95	17.41		$t_{80\%}$~4500h (80 ℃)	[19]
G-Timer-C6C8		0.899	25.32	79.34	18.07			
G-Timer-C8C10[a]		0.911	25.40	79.49	18.39		$t_{90\%}$~4500h (80 ℃)	
G-Timer-C8C10[b]		0.896	26.75	79.30	19.01		$t_{90\%}$~4500h (80 ℃)	
DIBP3F-Se	PM6	0.917	25.92	76.10	18.09	0.509	$t_{80\%}$~22 days (85 ℃)	[20]
DIBP3F-S		0.901	24.86	72.00	16.11	0.527	$t_{80\%}$~13 days (85 ℃)	
Tri-Y6-OD	PM6	0.916	25.30	77.8	18.03		$t_{80\%}$~1523 h (1 sun)	[21]

Tri-DT		0.943	23.89	77.4	17.44			
BT-BTz-BT		0.928	23.61	74.3	16.28			
BO-C11-BO		0.951	21.05	73.4	14.69			
EV-i	PM6	0.897	26.60	76.56	18.27		$t_{90\%}$~800 h (1 sun)	[22]
EV-o		0.957	6.20	42.13	2.50			
DY		0.959	22.01	70.50	14.88		$t_{94\%}$~12 h (90 ℃)	
TY	PM6	0.953	23.35	73.36	16.32		$t_{96\%}$~12 h (90 ℃)	[23]
QY		0.937	23.20	71.15	15.47		$t_{97\%}$~12 h (90 ℃)	
DYSe-1	PM6	0.885	27.51	76.6	18.56	0.520	$t_{80\%}$~500 h (65 ℃)	[24]
DYSe-2		0.884	27.45	75.2	18.22	0.522	$t_{80\%}$~500 h (65 ℃)	
BDY-α		0.869	26.09	76.68	17.38		$t_{90\%}$~1200 h (85 ℃)	
BDY-β	PM6	0.881	26.49	77.67	18.12		$t_{93\%}$~1200 h (85 ℃)	[25]
BTY		0.864	27.06	78.01	18.24		$t_{95\%}$~1200 h (85 ℃)	
HDY-m-TAT		0.915	23.33	67.8	14.42			
FDY-m-TAT	PM6	0.911	26.47	74.7	18.07			[26]
HDY-o-TAT		0.933	23.07	70.7	15.23			
FDY-o-TAT		0.914	25.14	73.6	16.91			
DYT		0.948	24.16	75.00	17.20		$t_{80\%}$~2157 h (1 sun)	
TYT-L	D18	0.968	24.19	75.00	17.47			[27]
TYT-S		0.964	25.18	77.00	18.61		$t_{80\%}$~2604 h (1 sun)	
DP-BTP	D18	0.96	22.73	69.10	15.08	0.42		[28]
Dimer-Qx	PM6	0.933	22.57	69.26	14.59		$t_{80\%}$~11261 h (80 ℃)	[29]
Dimer-2CF		0.900	26.39	80.03	19.02		$t_{80\%}$~11983 h (80 ℃)	
DYV	D18	0.915	24.90	75.20	17.38		$t_{80\%}$~24000 h (1 sun)	[30]
DYFV		0.897	25.50	77.40	17.88		$t_{80\%}$~45000 h (1 sun)	
2Y-wing		0.850	27.66	75.4	17.73		$t_{90\%}$~200 h (80 ℃)	
2Y-core	D18	0.864	10.58	61.5	5.63		$t_{67\%}$~200 h (80 ℃)	[31]
2Y-end		0.948	22.39	68.5	14.46		$t_{32\%}$~200 h (80 ℃)	
Tet-0		0.914	23.95	76.0	16.63		$t_{80\%}$~1436 h (1 sun)	
Tet-1	PM6	0919	24.53	76.8	17.32		$t_{80\%}$~1706 h (1 sun)	[32]
Tet-3		0.921	24.21	75.9	16.92		$t_{80\%}$~1546 h (1 sun)	
DY-P2EH	PM6	0.905	24.03	78.58	17.09		$t_{80\%}$~1100 h (85 ℃)	[33]

DYTVT	D18	0.97	24.13	74.0	17.39		
DYTCVT		0.94	23.66	76.0	16.96	$t_{80\%}$~2910 h (1 sun)	[34]

[a] PEDOT:PSS as the hole transport layer.

[b] 2PACz as the hole transport layer.

Table S5. Summary of contact angles (θ), surface tensions (γ), and Flory–Huggins interaction parameters (χ) for PM6 and four GMAs films.

Surface	θ_{water} (°) [a]	$\theta_{1\text{-Bromnaphthalene}}$ (°) [a]	γ (mN m^{-1})	$\chi^{D\text{-}A}$ [b]
PM6	101.30	45.02	32.62	-
GMA-SSS	96.57	35.12	37.15	0.149
GMA-SSeS	95.43	37.97	36.16	0.091
GMA-SeSSe	97.72	35.68	36.83	0.127
GMA-SeSeSe	97.69	33.88	37.53	0.174

a) Average θ_{water} and $\theta_{1\text{-Bromnaphthalene}}$ values were obtained from 5 individual measurements.

b) The Flory–Huggins interaction parameter between the donor (D) and acceptor (A) is calculated through the equation of $\chi = (\gamma_D^{1/2} - \gamma_A^{1/2})^2$.

Table S6. GIWAXS characteristics of four blend films, PM6:GMA-SSS, PM6:GMA-SSeS, PM6:GMA-SeSSe and PM6:GMA-SeSeSe.

		adscription	**q (Å^{-1})**	**d (Å)[a]**	**FWHM (Å^{-1})**	**L_c (Å)[b]**
PM6:GMA-SSS	OOP (100)	D/A	0.316	19.883	0.245	23.081
	OOP (200)	D/A	0.614	10.233		
	OOP (300)	D	0.939	6.691		
	OOP (400)	D/A	1.247	5.039		
	OOP (010)	D/A	1.650	3.808	0.399	14.173
	IP (100)	D/A	0.294	21.371	0.189	29.920
	IP (200)	D/A	0.601	10.455		
	IP (400)	D/A	1.227	5.121	0.496	11.401
	IP (010)	D/A	1.652	3.803	0.535	10.570
PM6:GMA-SSeS	OOP (100)	D/A	0.316	19.883	0.237	23.860
	OOP (200)	D/A	0.614	10.233		
	OOP (300)	D	0.919	6.837		

	OOP (400)	D/A	1.263	4.975		
	OOP (010)	D/A	1.657	3.792	0.376	15.040
	IP (100)	D/A	0.299	21.014	0.185	30.567
	IP (200)	D/A	0.601	10.455		
	IP (400)	D/A	1.264	4.971	0.499	11.332
	IP (010)	D/A	1.682	3.736	0.426	13.274
PM6:GMA-SeSSe	OOP (100)	D/A	0.286	21.969	0.297	19.040
	OOP (200)	D/A	0.611	10.283		
	OOP (300)	D	0.932	6.742		
	OOP (400)	D/A	1.273	4.936		
	OOP (010)	D/A	1.661	3.783	0.390	14.500
	IP (100)	D/A	0.300	20.944	0.188	30.079
	IP (200)	D/A	0.598	10.507		
	IP (300)	D	0.942	6.670		
	IP (400)	D/A	1.234	5.092	0.373	15.161
	IP (010)	D/A	1.552	4.048	0.627	9.019
PM6:GMA-SeSeSe	OOP (100)	D/A	0.299	21.014	0.279	20.268
	OOP (200)	D/A	0.612	10.267		
	OOP (300)	D	0.934	6.727		
	OOP (400)	D/A	1.262	4.979		
	OOP (010)	D/A	1.653	3.801	0.400	14.137
	IP (100)	D/A	0.304	20.668	0.193	29.300
	IP (200)	D/A	0.615	10.217		
	IP (300)	D	0.927	6.778		
	IP (400)	D/A	1.236	5.083	0.378	14.960
	IP (010)	D/A	1.626	3.864	0.544	10.395

[a] The d-spacing estimated from the equation $d=2\pi/q$.

[b] The Coherent length estimated from the Scherrer's equation $L_c= 2\pi k/FWHM$, where k is a shape factor (here use 0.9).

Table S7. Voltage loss parameters of PM6:GMAs-based OSCs.

	E_g [eV][a]	qV_{OC}^{SQ} [eV]	qV_{OC}^{rad} [eV]	ΔE_1 [eV][b]	ΔE_2 [eV][c]	ΔE_3 [eV][d]	E_{loss}[eV][e]
PM6:GMA-SSS	1.448	1.184	1.111	0.264	0.072	0.267	0.603
PM6:GMA-SSeS	1.446	1.182	1.119	0.264	0.064	0.246	0.573
PM6:GMA-SeSSe	1.420	1.157	1.095	0.262	0.062	0.268	0.592
PM6:GMA-SeSeSe	1.420	1.157	1.095	0.262	0.063	0.280	0.605

[a] E_g is obtained from the derivative of the EQE edges.

[b] $\Delta E_1 = E_g - qV_{OC}^{SQ}$.

[c] $\Delta E_2 = qV_{OC}^{SQ} - qV_{OC}^{rad}$.

[d] $\Delta E_3 = -kT \ln(EQE_{EL})$.

[e] $E_{loss} = \Delta E_1 + \Delta E_2 + \Delta E_3$

[1] S. E. Root, M. A. Alkhadra, D. Rodriquez, A. D. Printz, D. J. Lipomi, *Chem. Mater.* **2017**, *29*, 2646-2654.

[2] M. Ghasemi, N. Balar, Z. Peng, H. Hu, Y. Qin, T. Kim, J. J. Rech, M. Bidwell, W. Mask, I. McCulloch, W. You, A. Amassian, C. Risko, B. T. O'Connor, H. Ade, *Nat. Mater.* **2021**, *20*, 525-532.

[3] Y. liang, D. Zhang, Z. Wu, T. Jia, l. l, H. Tang, L. Hong, K. Zhang, J. B. C, L. N, H. F, *Nat. Energy* **2022**, *7*, 1180–1190.

[4] W. Liu, J. Yuan, C. Zhu, Q. Wei, S. Liang, H. Zhang, G. Zheng, Y. Hu, L. Meng, F. Gao, Y. Li, Y. Zou, *SCI CHINA CHEM* **2022**, *65*, 1374-1382.

[5] H. Wang, C. Cao, H. Chen, H. Lai, C. Ke, Y. Zhu, H. Li, F. He, *Angew. Chem. Int. Ed. Engl.* **2022**, *61*, e202201844.

[6] L. Zhang, Z. Zhang, D. Deng, H. Zhou, J. Zhang, Z. Wei, *Adv. Sci.* **2022**, *9*, 2202513.

[7] Y. Bai, Z. Zhang, Q. Zhou, H. Geng, Q. Chen, S. Kim, R. Zhang, C. Zhang, B. Chang, S. Li, H. Fu, L. Xue, H. Wang, W. Li, W. Chen, M. Gao, L. Ye, Y. Zhou, Y. Ouyang, C. Zhang, F. Gao, C. Yang, Y. Li, Z. G. Zhang, *Nat. Commun.* **2023**, *14*, 2926.

[8] H. Chen, Z. Zhang, P. Wang, Y. Zhang, K. Ma, Y. Lin, T. Duan, T. He, Z. Ma, G. Long, C. Li, B. Kan, Z. Yao, X. Wan, Y. Chen, *Energy Environ. Sci.* **2023**, *16*, 1773.

[9] H. Chen, B. Kan, P. Wang, W. Feng, L. Li, S. Zhang, T. Chen, Y. Yang, T. Duan, Z. Yao, C. Li, X. Wan, Y. Chen, *Angew. Chem. Int. Ed. Engl.* **2023**, *62*, e202307962.

[10] H. Fu, M. Zhang, Y. Zhang, Q. Wang, Z. Xu, Q. Zhou, Z. Li, Y. Bai, Y. Li, Z. G. Zhang, *Angew. Chem. Int. Ed. Engl.* **2023**, *62*, e202306303.

[11] H. Jeon, K.-p. Hong, J.-W. Lee, D. Jeong, T. N.-L. Phan, H.-G. Lee, J. S. Park, C. Wang, S. Xuyao, Y.-H. Kim, B. J. Kim, *Chem. Mater.* **2023**, *35*, 9276-9286.

[12] J.-W. Lee, C. Sun, C. Lee, Z. Tan, T. N.-L. Phan, H. Jeon, D. Jeong, S.-K. Kwon, Y.-H. Kim, B. J. Kim, *ACS Energy Lett.* **2023**, *8*, 1344-1353.

[13] J.-W. Lee, C. Sun, T. N.-L. Phan, D. C. Lee, Z. Tan, H. Jeon, S. Cho, S.-K. Kwon, Y.-H. Kim, B. J. Kim, *Energy Environ. Sci.* **2023**, *16*, 3339-3349.

[14] S. Li, R. Zhang, M. Zhang, J. Yao, Z. Peng, Q. Chen, C. Zhang, B. Chang, Y. Bai, H. Fu, Y.

Ouyang, C. Zhang, J. A. Steele, T. Alshahrani, M. B. J. Roeffaers, E. Solano, L. Meng, F. Gao, Y. Li, Z. G. Zhang, *Adv. Mater.* **2023**, *35*, 2206563.

[15] Z. Li, Z. Zhang, H. Chen, Y. Zhang, Y. Q. Q. Yi, Z. Liang, B. Zhao, M. Li, C. Li, Z. Yao, X. Wan, B. Kan, Y. Chen, *Adv. Energy Mater.* **2023**, *13*, 2300301.

[16] C. Sun, J.-W. Lee, C. Lee, D. Lee, S. Cho, S.-K. Kwon, B. J. Kim, Y.-H. Kim, *Joule* **2023**, *7*, 416-430.

[17] C. Sun, J. W. Lee, Z. Tan, T. N. L. Phan, D. Han, H. G. Lee, S. Lee, S. K. Kwon, B. J. Kim, Y. H. Kim, *Adv. Energy Mater.* **2023**, *13*, 2301283.

[18] P. Tan, H. Chen, H. Wang, X. Lai, Y. Zhu, X. Shen, M. Pu, H. Lai, S. Zhang, W. Ma, F. He, *Adv. Funct. Mater.* **2023**, *34*, 2305608.

[19] C. Wang, X. Ma, Y.-f. Shen, D. Deng, H. Zhang, T. Wang, J. Zhang, J. Li, R. Wang, L. Zhang, Q. Cheng, Z. Zhang, H. Zhou, C. Tian, Z. Wei, *Joule* **2023**, *7*, 2386-2401.

[20] J. Wu, Z. Ling, L. R. Franco, S. Y. Jeong, Z. Genene, J. Mena, S. Chen, C. Chen, C. M. Araujo, C. F. N. Marchiori, J. Kimpel, X. Chang, F. H. Isikgor, Q. Chen, H. Faber, Y. Han, F. Laquai, M. Zhang, H. Y. Woo, D. Yu, T. D. Anthopoulos, E. Wang, *Angew. Chem. Int. Ed. Engl.* **2023**, *62*, e202302888.

[21] C. Zhang, J. Song, J. Xue, S. Wang, Z. Ge, Y. Man, W. Ma, Y. Sun, *Angew. Chem. Int. Ed. Engl.* **2023**, *62*, e202308595.

[22] H. Zhuo, X. Li, J. Zhang, S. Qin, J. Guo, R. Zhou, X. Jiang, X. Wu, Z. Chen, J. Li, L. Meng, Y. Li, *Angew. Chem. Int. Ed. Engl.* **2023**, *62*, e202303551.

[23] H. Zhuo, X. Li, J. Zhang, C. Zhu, H. He, K. Ding, J. Li, L. Meng, H. Ade, Y. Li, *Nat. Commun.* **2023**, *14*, 7996.

[24] Y. Bai, T. Chen, X. Ji, J. Wang, W. Zhao, S. Yuan, Y. Zhang, G. Long, Z. Zhang, X. Wan, B. Kan, Y. Chen, *Adv. Energy Mater.* **2024**, 2400938.

[25] B. Chang, Y. Zhang, C. Zhang, M. Zhang, Q. Wang, Z. Xu, Q. Chen, Y. Bai, H. Fu, S. Meng, L. Xue, S. Kim, C. Yang, Y. Yi, Z. G. Zhang, *Angew. Chem. Int. Ed. Engl.* **2024**, *63*, e202400590.

[26] Y. Ding, W. A. Memon, D. Zhang, Y. Zhu, S. Xiong, Z. Wang, J. Liu, H. Li, H. Lai, M. Shao, F. He, *Angew. Chem. Int. Ed. Engl.* **2024**, *63*, e202403139.

[27] J. W. Lee, C. Sun, J. Lee, D. J. Kim, W. J. Kang, S. Lee, D. Kim, J. Park, T. N. L. Phan, Z. Tan, F. S. Kim, J. Y. Lee, X. Bao, T. S. Kim, Y. H. Kim, B. J. Kim, *Adv. Energy Mater.* **2024**, *14*, 2303872.

[28] X. Liu, Z. Zhang, C. Wang, C. Zhang, S. Liang, H. Fang, B. Wang, Z. Tang, C. Xiao, W. Li, *Angew. Chem. Int. Ed. Engl.* **2024**, *63*, e202316039.

[29] M. Lv, Q. Wang, J. Zhang, Y. Wang, Z. G. Zhang, T. Wang, H. Zhang, K. Lu, Z. Wei, D. Deng, *Adv. Mater.* **2024**, *36*, 2310046.

[30] J. Peng, F. Meng, J. Cheng, X. Lai, M. Du, M. Huang, J. Zhang, F. He, E. Zhou, D. Zhao, B. Zhao, *ACS Appl. Mater.* **2024**, *16*, 7317-7326.

[31] F. Yi, M. Xiao, Y. Meng, H. Bai, W. Su, W. Gao, Z. F. Yao, G. Qi, Z. Liang, C. Jin, L. Tang, R. Zhang, L. Yan, Y. Liu, W. Zhu, W. Ma, Q. Fan, *Angew. Chem. Int. Ed. Engl.* **2024**, *63*, e202319295.

[32] C. Zhang, J. Song, L. Ye, X. Li, M. H. Jee, H. Y. Woo, Y. Sun, *Angew. Chem. Int. Ed. Engl.* **2024**, *63*, e202316295.

[33] M. Zhang, B. Chang, R. Zhang, S. Li, X. Liu, L. Zeng, Q. Chen, L. Wang, L. Yang, H. Wang, J. Liu, F. Gao, Z. G. Zhang, *Adv. Mater.* **2024**, *36*, 2308606.

[34] J. W. Lee, C. Sun, H. Jeon, T. H. Q. Nguyen, T. N. L. Phan, X. Bao, Y. H. Kim, B. J. Kim, *Adv. Funct. Mater.* **2024**, 2404569.